



# Fires in Amazonian Blackwater Floodplain Forests: Causes, Human Dimension, and Implications for Conservation

Tayane Costa Carvalho<sup>1</sup>, Florian Wittmann<sup>2</sup>, Maria Teresa Fernandez Piedade<sup>1</sup>, Angélica Faria de Resende<sup>1,3</sup>, Thiago Sanna Freire Silva<sup>4,5</sup> and Jochen Schöngart<sup>1\*</sup>

<sup>1</sup> Ecology, Monitoring, and Sustainable Use of Wetlands (MAUA), National Institute for Amazon Research (INPA), Coordination of Environmental Dynamics, Manaus, Brazil, <sup>2</sup> Wetland Ecology, Karlsruhe Institute for Technology (KIT), Institute for Geography and Geoecology, Rastatt, Germany, <sup>3</sup> Laboratory of Tropical Forestry (LASTROP), Department of Forest Sciences, “Luiz de Queiroz” College of Agriculture (ESALQ), University of São Paulo (USP), Piracicaba, Brazil, <sup>4</sup> Instituto de Geociências e Ciências Exatas, Universidade Estadual Paulista (UNESP), Rio Claro, Brazil, <sup>5</sup> Biological and Environmental Sciences, Faculty of Natural Sciences, University of Stirling, Stirling, United Kingdom

## OPEN ACCESS

### Edited by:

Guillermo Emilio Defossé,  
Consejo Nacional de Investigaciones  
Científicas y Técnicas (CONICET),  
Argentina

### Reviewed by:

Evgeny Abakumov,  
Saint Petersburg State University,  
Russia  
Valentina Bacciu,  
National Research Council (CNR), Italy

### \*Correspondence:

Jochen Schöngart  
jochen.schongart@inpa.gov.br

### Specialty section:

This article was submitted to  
Fire and Forests,  
a section of the journal  
Frontiers in Forests and Global  
Change

**Received:** 08 August 2021

**Accepted:** 08 November 2021

**Published:** 14 December 2021

### Citation:

Carvalho TC, Wittmann F,  
Piedade MTF, Resende AF, Silva TSF  
and Schöngart J (2021) Fires  
in Amazonian Blackwater Floodplain  
Forests: Causes, Human Dimension,  
and Implications for Conservation.  
Front. For. Glob. Change 4:755441.  
doi: 10.3389/ffgc.2021.755441

The Amazon basin is being increasingly affected by anthropogenic fires, however, most studies focus on the impact of fires on terrestrial upland forests and do not consider the vast, annually inundated floodplains along the large rivers. Among these, the nutrient-poor, blackwater floodplain forests (*igapós*) have been shown to be particularly susceptible to fires. In this study we analyzed a 35-year time series (1982/1983–2016/2017) of Landsat Thematic Mapper from the Jaú National Park (Central Amazonia) and its surroundings. Our overall objective was to identify and delineate fire scars in the *igapó* floodplains and relate the resulting time series of annual burned area to the presence of human populations and interannual variability of regional hydroclimatic factors. We estimated hydroclimatic parameters for the study region using ground-based instrumental data (maximum monthly temperature– $T_{max}$ , precipitation– $P$ , maximum cumulative water deficit– $MCWD$ , baseflow index– $BFI$ , minimum water level– $WL_{min90}$  of the major rivers) and large-scale climate anomalies (Oceanic Niño Index– $ONI$ ), considering the potential dry season of the non-flooded period of the *igapó* floodplains from September to February. Using a wetland mask, we identified 518,135 ha of *igapó* floodplains in the study region, out of which 17,524 ha (3.4%) burned within the study period, distributed across 254 fire scars. About 79% of the fires occurred close to human settlements (<10 km distance), suggesting that human activities are the main source of ignition. Over 92.4% of the burned area is associated with El Niño events. Non-linear regression models indicate highly significant relationships ( $p < 0.001$ ) with hydroclimatic parameters, positive with  $T_{max}$  ( $R^2_{adj.} = 0.83$ ) and the  $ONI$  ( $R^2_{adj.} = 0.74$ ) and negative with  $P$  ( $R^2_{adj.} = 0.88$ ),  $MCWD$  ( $R^2_{adj.} = 0.90$ ),  $WL_{min90}$  ( $R^2_{adj.} = 0.61$ ) and  $BFI$  ( $R^2_{adj.} = 0.80$ ). Hydroclimatic conditions were of outstanding magnitude in particular during the El Niño event in 2015/2016, which was responsible for 42.8% of the total burned floodplain area. We discuss these results under a historical background of El Niño occurrences and a political, demographic, and socioeconomic panorama

of the study region considering the past 400 years, suggesting that disturbance of *igapós* by fires is not a recent phenomenon. Concluding remarks focus on current demands to increase the conservation to prevent and mitigate the impacts of fire in this vulnerable ecosystem.

**Keywords:** *igapó*, El Niño, Interdecadal Pacific Oscillation, human occupation, Jaú National Park, Extractive Reserve Rio Unini, Negro River, hydroclimatic drought

## INTRODUCTION

The Amazon biome holds the largest amount of global continuous tropical forest cover, embedded in the largest river basin on Earth hosting a megadiversity in flora and fauna (ter Steege et al., 2020). Through biosphere-atmosphere interactions, the biota and hydrological and biogeochemical cycles are intrinsically related and in equilibrium, providing essential ecosystem services for human societies (Salati and Vose, 1984). However, there is significant uncertainty regarding the resilience and adaptability of Amazonian rainforests to increasing temperature and hydrometeorological extreme events (Barichivich et al., 2018; Marengo et al., 2018), massive disturbances caused by deforestation, increasing fire incidence, and intensified land-use change (Davidson et al., 2012; Aragão et al., 2018). This is mainly due to the complex and varying interactions and feedback loops between climate and land-use changes (Baker et al., 2021), the high spatiotemporal variability of climate and hydrology and associated driving forces (Marengo and Espinoza, 2016), and differences in soil and vegetation cover of the varying Amazonian ecosystems.

Most of our understanding of fire dynamics in the Amazon is related to non-flooded upland (*terra-firme*) forests (Cochrane, 2003; Alencar et al., 2015; Nobre et al., 2016; Barlow et al., 2020; Brando et al., 2020). Fires following deforestation to expand agriculture and livestock production as well as the implementation of large infrastructure such as road networks, mining activities, river dams for hydropower generation and urban footprints increased unprecedentedly in the Amazon basin during the last decades (Davidson et al., 2012; Aragão et al., 2018). Especially during severe hydroclimatic droughts, fires can escape, accidentally or intentionally, into adjacent *terra-firme* forests (Alencar et al., 2015; Barlow et al., 2020; Brando et al., 2020) and even floodplain forests (Reis et al., 2021), both outside and within protected areas (Nepstad et al., 2006; Silva et al., 2021). This occurs mainly towards the end of the dry season due to the cumulative effect of water deficit, which may expand into the wet season in regions influenced by El Niño (Nepstad et al., 2004; Schöngart et al., 2004; Aragão et al., 2007; Alencar et al., 2015). Despite the interannual variability related to the El Niño-Southern Oscillation (ENSO), climate oscillations with low frequency, such as the Interdecadal Pacific Oscillation (IPO), and Pacific Decadal Oscillation (PDO), shape the multidecadal pattern of rainfall and hydrological regimes in the Central, Northern and Eastern Amazon (Marengo, 2004, 2009; Aragão et al., 2018; Barichivich et al., 2018; Granato-Souza et al., 2020). Both low-frequency oscillations are characterized by sea surface temperature (SST) anomaly patterns similar to

ENSO but in a decadal mode of changing warm and cold phases with cycles of 40–60 years (Henley, 2017). The PDO covers the Northern and Equatorial Pacific, while the IPO has a tripole pattern also covering the Southern Pacific, however, both oscillations are directly correlated (Henley, 2017). Several studies indicate that teleconnections between El Niño and precipitation in South America are strengthened during the warm phase of the IPO (PDO) (Andreoli and Kayano, 2005; Wang and Liu, 2016; Campozano et al., 2020; Nguyen et al., 2021).

Very little, however, is currently known about fire dynamics in Amazonian wetland environments, which cover more than 30% of the Amazon basin (Junk et al., 2011). Anthropogenic fires may be a further stressor on these vulnerable environments, which are known to be highly impacted by hydrological changes from increased climate variability (Gloor et al., 2015) and hydropower damming (Schöngart et al., 2021). The few existing studies regarding fire and Amazonian floodplain vegetation focus mainly on oligotrophic blackwater floodplains (*igapó*), which are particularly vulnerable to fires due to slow dynamical processes (Resende et al., 2014; Flores et al., 2017; Schöngart et al., 2017; Flores and Holmgren, 2021). *Igapós* cover more than 119,000 km<sup>2</sup> of the Negro River basin, occurring along large and small blackwater rivers draining the deeply weathered Pre-cambrian formations of the Guyana Shield mainly extending across the northern, central, and eastern regions of the Amazon basin (Junk et al., 2015; Wittmann and Junk, 2016). In the large river catchments, the rainfall seasonality results in regular and predictable flood pulses with one high and low water period during the year, alternating between aquatic and terrestrial phases in the Central Amazonian floodplains (Junk et al., 2011). The monomodal flood pulse is the main driver of geomorphological processes and biogeochemical cycles, as well as of biological life cycles and growth rhythms (Junk et al., 1989). *Igapós* are mainly covered by forests (>85% of the area) with varying structure and diversity along hydroedaphic gradients (Wittmann et al., 2010; Montero et al., 2014; Targhetta et al., 2015; Lobo et al., 2019). For the *igapós* of the Negro River basin, a total of 449 valid tree species have been recorded to date with distribution patterns mainly shaped by the flooding regime (Householder et al., 2021) to which tree species have adapted over evolutionary timescales (Wittmann et al., 2010), developing flood-specific adaptations at morpho-anatomical, physiological, and biochemical levels (Junk, 1989; De Simone et al., 2002; Parolin et al., 2004; Haase and Rättsch, 2010; Piedade et al., 2010).

*Igapós* along the Negro River basin and other Guyana Shield tributaries are affected by hydrometeorological droughts induced by severe El Niño events that coincide with the river's low-water period (Labat et al., 2012; Flores et al., 2014). Although the

topsoil of most *igapó* forests (mainly Gleysols and hydromorphic Podzols; Sombroek, 1984) is generally characterized by silty and clayish substrate of some decimeter thickness (Furch and Junk, 1997; Aguiar, 2015), the soil bedding is predominantly sandy (Latrubesse and Franzinelli, 2005) with low water-retention capacity during the dry period. In general, *igapó* forests are composed by a higher proportion of deciduous tree species compared to *terra-firme* forests (Haugaasen and Peres, 2005), which shed leaves mainly during the flooding period (Schöngart et al., 2002; Parolin et al., 2010). Due to the oligotrophic conditions, many tree species have sclerophyllous leaves (Waldhoff and Furch, 2002), leading to a comparatively slow decomposition due to a combination of elevated levels of structural carbohydrates and low nutrient contents (Irmiler and Furch, 1980; Furch and Junk, 1997). Leaf decomposition is further reduced by the anoxic conditions resulting from long-lasting inundations leading to a low diversity and/or periodic elimination of soil invertebrates (Irmiler and Furch, 1980; Wantzen et al., 2008; Adis et al., 2010). These factors generate accumulation of fine litter covering the alluvial substrate of *igapó* forests (Kauffman et al., 1988; Santos and Nelson, 2013). As a consequence of the nutrient-poor soil conditions, a mat of fine roots near or on top of the soil surface establishes (Meyer et al., 2010). Litter and aboveground root mats form an enormous layer of fine fuel, which is about twice as large than in *terra-firme* forests (Santos and Nelson, 2013). A comparatively low canopy and open understory characterizes particularly highly flooded topographies, where high radiation incidence results in a dry microclimate at and near the forest floor (Carvalho, 2019). According to Uhl et al. (1988), ignition of fine fuel is favored when relative air humidity is below 65%, which frequently occurs in *igapó* forests (Resende et al., 2014; Almeida et al., 2016). As dead leaves are a dry fuel with high combustion heat (Hughes, 1971; Rivera et al., 2012), understory fires spread rapidly along the soil surface, killing the surface-near fine roots, resulting in massive tree mortality (Resende et al., 2014; **Supplementary Figure 1**). Moreover, slow recovery times keep burnt areas open for several years, further exposing them to recurring fires (Flores et al., 2016; Flores and Holmgren, 2021).

Although the mechanism that turn *igapós* vulnerable to fires are quite well understood, we emphasize in this study on the regional hydroclimatic conditions generated by El Niño with the hypothesis that fires in the *igapó* occur mainly under severe hydroclimatic drought conditions associated with El Niño events during warm IPO phases. Therefore, we mapped fire scars in the *igapós* of the Jáu National Park (JNP) and an 8-km wide buffer zone, located in the lower Negro River basin (Central Amazonia) by remote sensing techniques (Landsat TM, ETM+, and OLI sensors) along 35 years (1982/1983 to 2016/2017). The annually burnt floodplain forests were related to regional climate and hydrological parameters of the main rivers in the study region and large-scale SST anomalies from the equatorial Pacific as a measure for El Niño episodes. In the following, we focus on the role of human populations in this ecosystem, who are thought to be the main ignition source of understory fires (Ritter et al., 2012), which is so far poorly acknowledged in previous studies. In order to test the hypothesis of human presence as main ignition, we analyzed fire occurrence in the nowadays mainly protected *igapó*

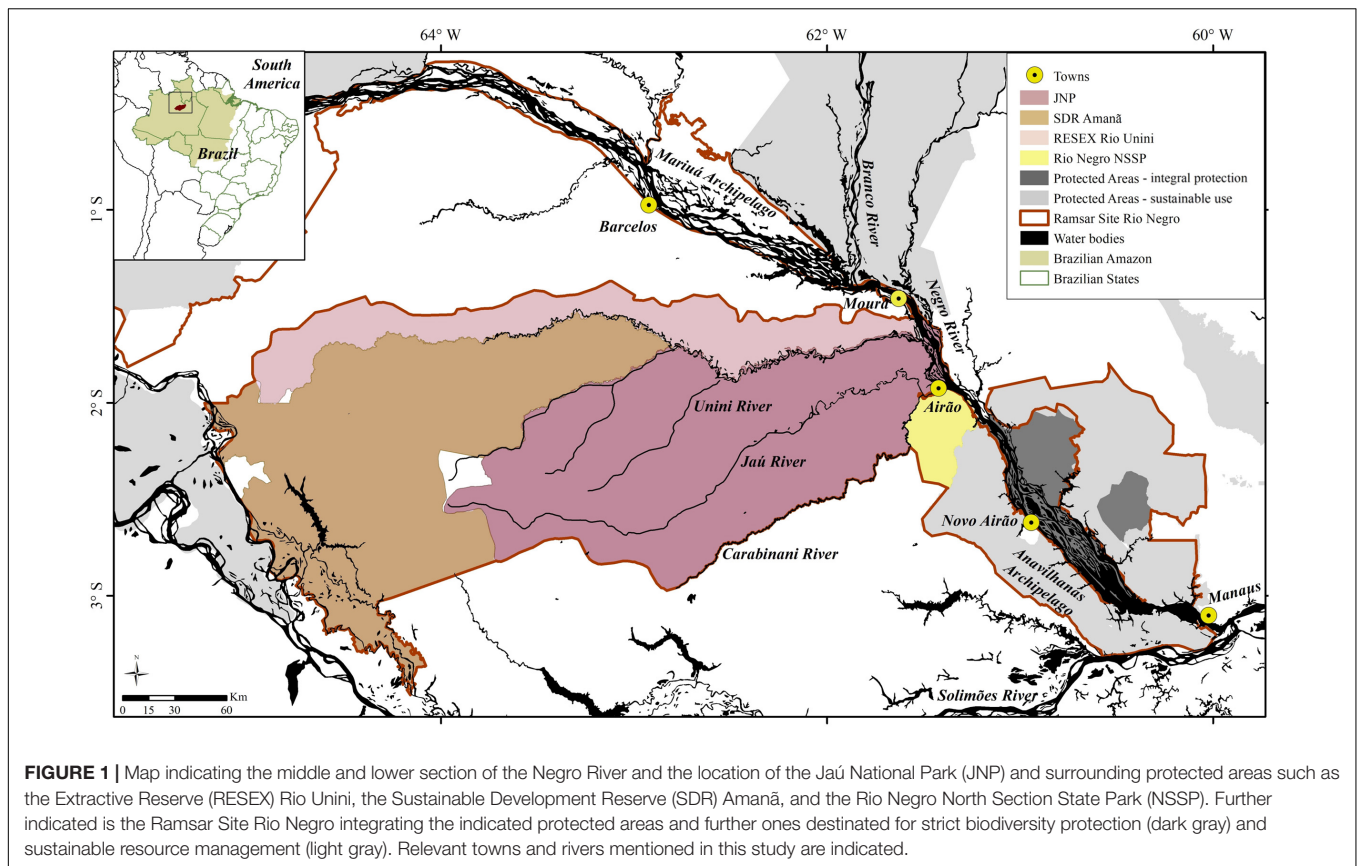
considering human settlements in the studied region and period. Based on our findings, we then raise the hypothesis that fire disturbance also occurred in the past due to severe hydroclimatic droughts generated by El Niño conditions, but human presence reinforced ignition. More specifically, our hypothesis is that past fire disturbances in the *igapó* intensified mainly in those periods influenced by frequent El Niño events during warm IPO phases and characterized by intensive human occupation and natural resource extraction. Therefore, we draw a historical background considering social, cultural, economic and political aspects of human occupation in the study region comprising the last 400 years based on a literature review. In a next step we linked the historical panorama with the occurrence of past El Niño events and warm IPO phases obtained from available reconstructions based on tree-ring networks and ice cores. Building a bridge between provided insights of past fire disturbances in *igapós* with the current scenario of the protected study region, we draw our conclusions focused on the dynamics and conservation of this vulnerable ecosystem in the study region and the Negro River basin considering the current status of protected areas.

## MATERIALS AND METHODS

### Study Region

The Jáu National Park (JNP) was created in September 1980 (Federal Decree 85.200) and is located between the municipalities of Barcelos and Novo Airão of the state of Amazonas, 220 km distant in northwest direction from Manaus (**Figure 1**). JNP is one of the largest National Parks in Brazil, covering 2,272,000 hectares and is inserted in a mosaic of state and federal conservation units. The limits of the southern edge of the park extend to the Carabinani River, forming the border with the Rio Negro State Park North Section. The northern portion is limited by the Unini River forming the border with the Extractive Reserve (RESEX) Rio Unini. Toward the east the JNP reaches the Negro River and toward the west the Amanã Sustainable Development Reserve. The JNP, together with the Sustainable Development Reserves Amaña and Mamirauá, and the Anavilhanas National Park, form the Central Amazonian Conservation Complex, declared by UNESCO as World Heritage Site in 2000.

The lower Negro River up to the confluence with the Branco River (**Figure 1**) is strongly influenced by the backwater effect of the mainstem (Amazonas-Solimões) (Meade et al., 1991). The backwater effect also extends to the lower sections of the Unini, Jáu and Carabinani rivers until the first rapids in each river (**Figure 2**). Hydrographic conditions in this region are similar in the timing of maximum (June) and minimum (October/November) water levels and flood amplitude (about 10 m) in comparison to the water level record of Manaus (Schöngart and Junk, 2007). About 70% of the JNP is covered by dense upland forests (*terra-firme*) while *igapó* forests comprise about 12% and white-sand ecosystems (*campinarana*) another 10% with some palm swamps dominated by *Mauritia flexuosa* (*buritizal*) in interfluvial regions (Borges et al., 2001). The relief is flat with some hilly areas of up to 150 m above average sea level cut by large valleys with *igapó* floodplains. Dominating



soil types in the JNP are orthic Acrisols and hydromorphic Laterites and Podzols (FVA, 1998). Almost 86% of the JNP is destined for strict protection of biodiversity covering all main vegetation types, while about 14% is destined for residence, resource extraction and small-scale agriculture of the human population mainly occurring in *igapós* and adjacent *terra-firme* forests along the middle and lower section of the Jaú and Unini rivers (FVA, 1998).

With the creation of the RESEX Rio Unini in 2007 (Law No. 11,516) a management plan was implemented defining zones for different land-use intensities and biodiversity protection (ICMBio, 2014). Areas destined for intensive community use (about 3,000 ha) are located in the eastern part of the conservation unit at the river margins close to the confluence with the Negro River, allowing settlements, livestock production and small-scale agriculture, including the use of fire (ICMBio, 2014). The zone for management of natural resources (extraction of timber and non-timber forest products and fishing) comprises an area of approximately 340,000 ha and extend mainly along the lower and middle course of the Unini River, including *igapó* floodplains. Areas destined for strict biodiversity protection (about 524,000 ha) are located in the western part of the RESEX Rio Unini, integrating mainly *campinarana*, *terra-firme* and *igapó* in the headwaters of the Unini River and its tributaries (ICMBio, 2014).

Both, the JNP and RESEX Rio Unini are integrated with other 18 conservation units in the Ramsar Regional Site Rio

Negro, created in March 2018, covering an area of more than 12 million hectares (Figure 1). The Ramsar Convention on Wetlands of International Importance provides a framework for the conservation and wise use of these ecosystems and their natural resources based on national inventories to establish specific conservation strategies (Wittmann et al., 2015). The Ramsar Regional Site Rio Negro extends along the middle and lower sections of the Negro River basin and interfluvial regions between the Negro and Japurá rivers. It integrates important oligotrophic wetlands such as *igapó* floodplains, among them the two largest freshwater archipelagos on Earth (Mariuá and Anavilhanas) (Latrubesse and Stevaux, 2015), *campinarana* and interfluvial palm swamps (*buritizal*).

## Historical Background of Human Occupation in the Study Region

In this section, we provide a summary of the demographic and socioeconomic background of the study region, as this information is essential for the later discussion about the relationship of *igapó* fires and human presence in a historical context (for more detailed information, see **Supplementary Material**). Humans have been present in the study region since the late Holocene, reflected by hundreds of petroglyphs at the JNP and RESEX Rio Unini (Valle, 2012). The foundation of Santo Elias do Jaú by Carmelite missionaries in 1694 (named Airão in 1759), located close to the mouth of the Jaú River (Figure 1),

was the beginning of a profound sociocultural transformation of the indigenous populations in the study region (Leonardi, 1999). During the 18th century, the native population was decimated by conflicts, slavery, and diseases, or used as labor for resource extraction. The first half of the 19th century is characterized by economic and demographic decline of the region and massive decimation of the native and descendant population (Leonardi, 1999; Sampaio, 2003). During the second half of the 19th century, Airão gained economic importance, especially with the beginning of the rubber boom, when thousands of immigrants from the Brazilian Northeast settled along the Jaú, Carabinani, and Unini rivers (Leonardi, 1999). The collapse of the rubber boom in the 1920s caused again a progressive demographic decline in the study region which continued after the establishment of the JNP in 1980 since people are not allowed to reside in this category of protected area (SNUC Law 9.985/2000). This conflict is still not resolved, as traditional populations lived in the region long before the establishment of the JNP. The demographic census of 2001 indicates around 377 residents in the JNP and about 669 residents along the lower section of the Unini River (Pinheiro and Macedo, 2004).

## Remote Sensing Data

For the remote sensing analyses we considered the JNP and an 8-km wide buffer zone, integrating the *igapós* along the blackwater rivers forming the border of the protected area comprising in total 3,072,295 ha (Figure 2). Using the wetland

mask of Hess et al. (2015), a total of 518,135 ha *igapó* floodplain forests were identified, corresponding to 17% of the area. Of those, about 70% (363,420 ha) were located inside the JNP and 30% (154,715 ha) in the buffer zone. The reconstruction of fire occurrences in the study region covered the period from 1984 to 2017. The fires were identified from images obtained by Thematic Mapper (TM), Enhanced Thematic Mapper Plus (ETM+), and Operational Land Imager (OLI) aboard the Landsat 5, 7 and 8 satellites, respectively, with a spatial resolution of 30 meters. Images were made available by the United States Geological Survey (USGS) of NASA by the website Earth Explorer<sup>1</sup> of collection 1 (Higher level science data – Level 2 – on demand) with pixel values already corrected for surface reflectance. The study area is included in scenes 232/61; 232/62; 233/61 and 233/62, Datum WGS84, designed in the Universal Transverse Mercator Projection (UTM) zone 20S. The detection and delimitation of fire scars were carried out following the method proposed by Alvarado et al. (2017). For this purpose, false color fusion compositions were generated using the mid-infrared (SWIR), near-infrared (NIR) and red (R) bands in the red, green, and blue (RGB) channels. The bands used were 5-4-3 for the TM and ETM+ sensors, and bands 6-5-4 for the OLI sensor, obtaining composite images in false RGB color with fixed contrast levels to minimize misinterpretation due to fluctuations in reflectance intensity.

<sup>1</sup><http://earthexplorer.usgs.gov>

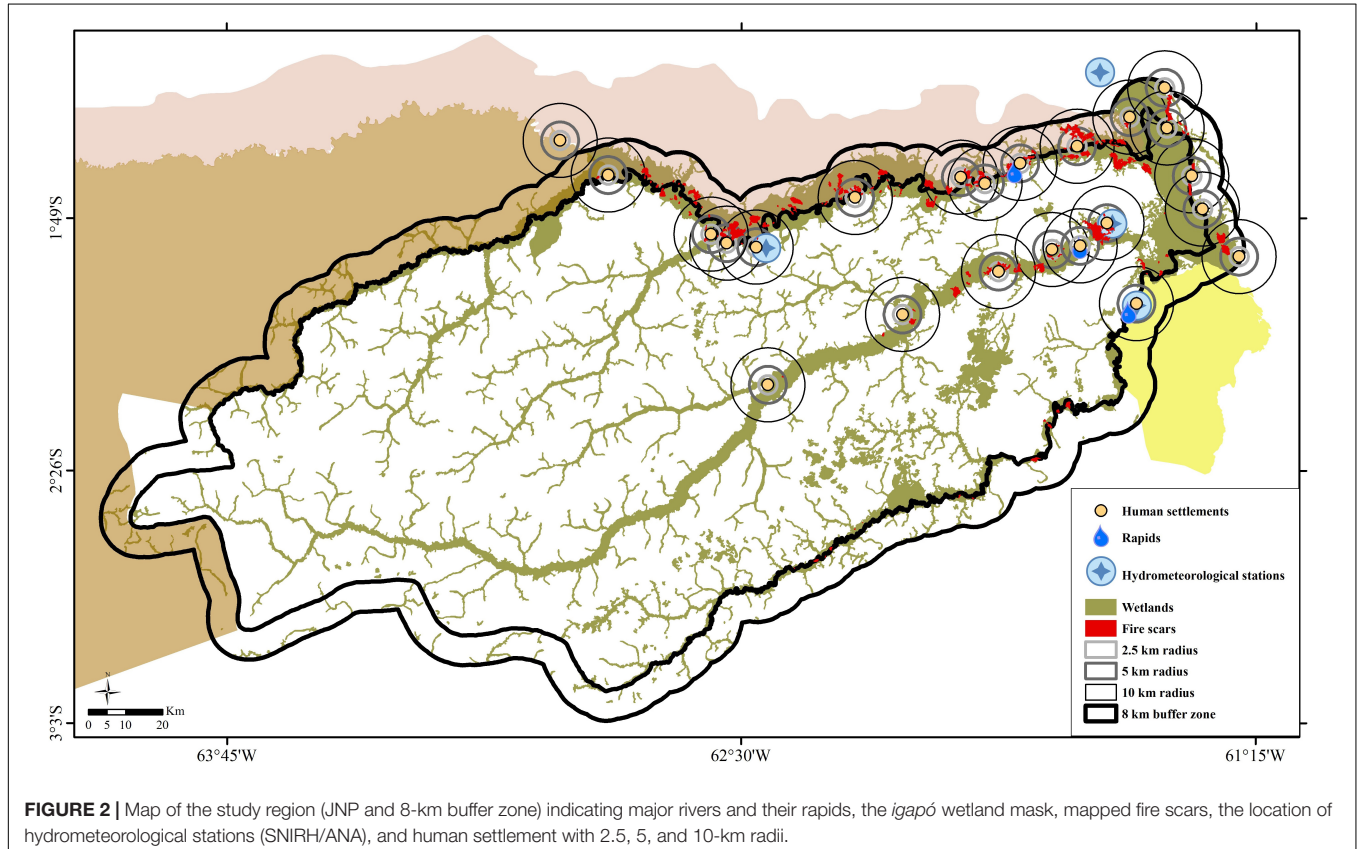


**FIGURE 2 |** Map of the study region (JNP and 8-km buffer zone) indicating major rivers and their rapids, the *igapó* wetland mask, mapped fire scars, the location of hydrometeorological stations (SNIRH/ANA), and human settlement with 2.5, 5, and 10-km radii.

The delimitation of the burned areas was then performed by visual interpretation and manual vectorization of the fire scars, with a standardized cartographic scale of 1:25,000. For the composition of the images, the R software (R Core Team, 2018) was used through the “raster” (Hijmans and van Etten, 2013) and “rgdal” (Bivand et al., 2014) packages for the vectorization of scars. For the reprojection of the images, we applied ArcGIS 10.4 software. The fire scars mapped in the January 1984 image were attributed to fires that occurred in the period 1982/1983, as despite the lack of Landsat images prior to 1984, the mortality of post-fire trees in the *igapó* forests is usually visible for a few weeks or months after the fire. Fires were classified according to the size of the burned area (<4 ha; 4.1–40 ha, 40.1–100 ha; >100 ha) to assess the extent of the fire in relation to hydroclimatic conditions and human occupation. Areas which burnt at least twice during the monitored period were analyzed considering the location, burnt area, year and frequency of recurring fire events on previously burnt areas. Based on these data we calculated the mean and standard deviation of the return interval and the percentage of the originally burnt area. To evaluate the anthropic factor on fire occurrence in the JNP and its surroundings, we applied three concentric zones with 2.5 km (intensive land use), 5 km (extensive land use) and 10 km (remote land use) around the settlements (Heckenberger et al., 2008). Therefore, the geographic coordinates of each settlement in the study region were placed on the map of fire scars, considering the three radii to count the number of fire scars. For this process, ArcGIS 10.4 software was used.

## Climate and Hydrographic Data

In contrast to the non-flooded upland forests (*terra-firme*), where climatic water deficit is mainly related to rainfall seasonality, the Central Amazonian *igapó* presents a more complex regime. The regular and annual flood pulse in the Central Amazonian *igapó* generally extends from the middle of the rainy season (around March) to the middle of the dry season with a 3-months shift compared to the precipitation regime (Schöngart et al., 2002). This has strong implications for the climatic water deficit in this environment, which generally remains flooded during the first months of the dry season. For our research approach we therefore considered the period from September to February as terrestrial phase, which is representative for the majority of *igapó* forests in the study region (Carvalho, 2019). During this period *igapó* floodplains become susceptible to fire due to climatic water deficit, especially in periods of El Niño occurrences, which decrease precipitation during the early rainy season (Aragão et al., 2007), leading to an extension of the non-flooded period in Central Amazonian floodplains into the wet season (Schöngart and Junk, 2007).

Monthly data for mean ( $T_{mean}$ ), minimum ( $T_{min}$ ) and maximum ( $T_{max}$ ) temperature were obtained from the Brazilian National Institute for Meteorology (INMET) for the stations Manaus (located about 200 km in SE direction) and Barcelos (located about 150 km in NE direction) (Figure 1) for the period 1982–2017 (Supplementary Table 1), as no ground-based data

were available for the study region. Monthly and annual averages and standard deviations were calculated for  $T_{mean}$ ,  $T_{min}$  and  $T_{max}$  based on mean values from the records of Manaus and Barcelos.

Based on the temperature record, the potential evapotranspiration ( $ET_{pot}$ ) was estimated using the equation suggested by Thornthwaite (1948):

$$ET_{pot} = 1.6(10 \times T_{mean}/I)^a \quad (1)$$

where,  $ET_{pot}$  is the monthly potential evapotranspiration (cm),  $T_{mean}$  is the monthly mean temperature (°C),  $I$  represents a heat index calculated by the sum of the 12 monthly mean temperatures  $i$  as follows:

$$i = (T_{mean} \div 5)^{1.514} \quad (2)$$

The parameter  $a$  is computed by the following equation (Ribeiro and Villa Nova, 1979):

$$a = 6.75 \times 10^{-7} \times I^3 - 7.71 \times 10^{-5} + I^2 1.79 \times 10^{-2} \times I + 0.49 \quad (3)$$

Monthly precipitation data were obtained from the Hidroweb platform of the National Water Resources Information System (SNIRH) operated by the Brazilian National Water Agency (ANA) and the Geological Survey of Brazil (CPRM) (for more details, see Supplementary Table 1). Three stations situated within (Baruri, Umanapana, and Seringalzinho) (Figure 2) or nearby (Moura, Novo Airão) the study region (Figure 1) were used to calculate average and standard deviation of monthly and annual precipitation from July 1982 to June 2017. The maximum cumulative water deficit ( $MCWD$ ) was estimated to represent annual climatological drought intensity during the terrestrial phase of the *igapó* floodplains (September to February) from 1982/1983 to 2016/2017. For  $MCWD$ , monthly values with  $ET_{pot} >$  precipitation (water deficit) were accumulated during all months of the terrestrial phase (Aragão et al., 2007; Anderson et al., 2018).

As a measure of the El Niño-Southern Oscillation (ENSO) we used the Ocean Niño Index ( $ONI$ ). The  $ONI$  is a 3-month running mean of SST anomalies (ERSST.v5; Huang et al., 2017) in the Niño 3.4 region (5°N–5°S/120°–170°W) based on a 30-year base period (1986–2015) (Supplementary Table 1). Based on the 3-month periods November–December–January (NDJ) and DJF, El Niño events were classified into weak ( $ONI \geq 0.5$  and  $< 1.0^\circ\text{C}$ ), intermediate ( $ONI \geq 1.0$  and  $< 1.5^\circ\text{C}$ ) and strong ( $ONI \geq 1.5^\circ\text{C}$ ) episodes. Data were obtained by the Climate Prediction Center of the U.S. National Oceanic and Atmospheric Administration (NOAA)<sup>2</sup>.

Data of daily water levels were obtained from four stations available on the Hidroweb platform (SNIRH/ANA) for the Jaú, Carabinani and Unini rivers within the study region, and for the Negro River at Moura, nearby the JNP (for more details, see Supplementary Table 1). The hydrological year was defined from 1st July to 30th June of the subsequent year comprising the period between the regularly occurring

<sup>2</sup>[https://origin.cpc.ncep.noaa.gov/products/analysis\\_monitoring/ensostuff/ONI\\_v5.php](https://origin.cpc.ncep.noaa.gov/products/analysis_monitoring/ensostuff/ONI_v5.php)

maximum water levels from 1982 to 2017. Missing data for period less than one month were interpolated. Applying the method of indicators of hydrologic alteration (Richter et al., 1996), baseflow index (*BFI*; 7-day minimum water level divided by the annual mean water level), and 90-day minimum water level ( $WL_{min90}$ ) were calculated as a measure of the hydrological drought in the *igapó* floodplains. Therefore, we calculated average and standard deviation of the available data of daily water levels from the four hydrological stations, setting the absolute minimum water level of each time series to zero (Supplementary Figure 2).

For the reconstruction of past El Niño events we obtained SST anomalies for DJF of the Niño 3.4 region ( $>0.5^{\circ}\text{C}$ ) based on instrumental data (HadISST monthly SST data set from 1870 to 2016; Rayner et al., 2003) and the reconstruction of Cook et al. (2018) for the last 400 years, based on tree-ring chronology networks of the Eastern Australia New Zealand Drought Atlas (Palmer et al., 2015) and Mexican Drought Atlas (Stahle et al., 2016). We associated the occurrence of past El Niño events with instrumental (Henley, 2017) and reconstructed warm IPO phases for the past four centuries. The reconstructions of the IPO phases are based on tree-ring records from Vietnam and the North American Drought Atlas (Buckley et al., 2019) and an assemblage of four ice cores around the Pacific basin (Porter et al., 2021).

## Data Analyses

The total annual burnt *igapó* area and the hydroclimatic variables were tested for normal distribution by a Shapiro-Wilk test. With exception of the annual burnt area and the *MCWD* all hydroclimatic variables present a near normal distribution ( $p > 0.05$ ). Hydroclimatic parameters were compared between years with fire occurrence and those without burning, as well as the hydroclimatic conditions between El Niño episodes and other years, using the non-parametric Mann-Whitney *U* test (R Core Team, 2018). Trends of hydroclimatic data during the study period were analyzed applying the non-parametric Mann-Kendell test (Pohlert, 2020), commonly used in detecting trends of meteorological and hydrological variables (Ahn and Merwade, 2014). The generated positive (negative) *Z*-values indicated increasing (decreasing) trends. For the terrestrial phase, average ( $T_{max}$ , *ONI*), cumulative (*P*, *MCWD*) and single values (*BFI*,  $WL_{min90}$ ) were correlated to the annual burnt *igapó* area from 1982/1983 to 2016/2017 by non-linear regression models:

$$\text{Burnt area} = a + \exp(c \times (X - b)) \quad (4)$$

where, *X* represents the hydroclimatic parameters  $T_{max}$ , *ONI*, *P*, *MCWD*, *BFI* or  $WL_{min90}$ , and *a*, *b* and *c* the coefficients of the exponential equations with positive (negative) values for *c* turning them into growth (decay) functions (X-Act 7.0, SciLab).

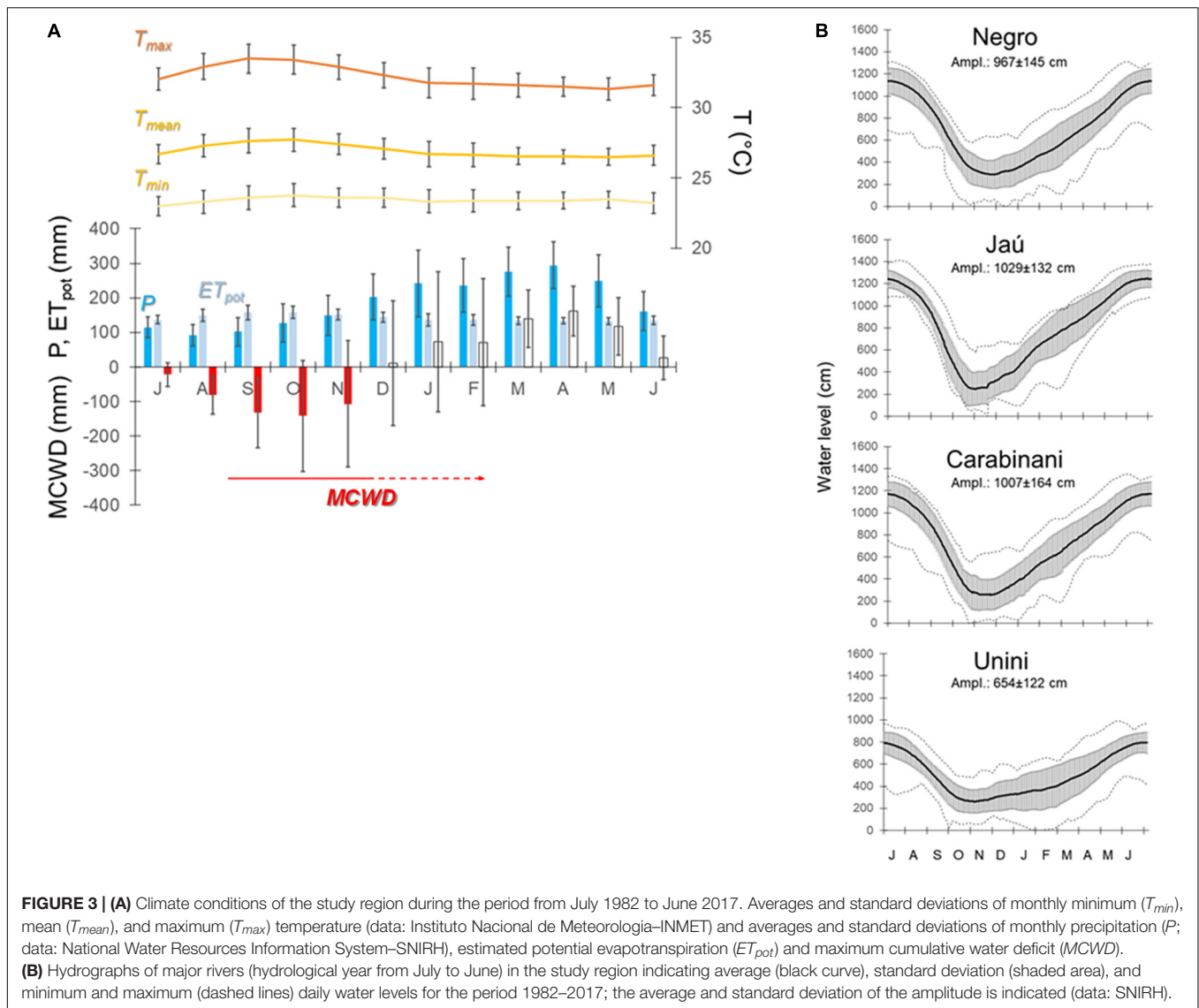
## RESULTS

### Climate and Hydrography of the Study Region

The climate in the region during the analyzed period was characterized by average annual precipitation of  $2,362 \pm 273$  mm (standard deviation) (Figure 3). Maximum monthly rainfall occurred in April ( $294 \pm 68$  mm) with only August demonstrating monthly precipitation of less than 100 mm ( $92 \pm 32$  mm). The estimates for monthly potential evapotranspiration ( $ET_{pot}$ ) varied on average between 133 and 158 mm, indicating a period of climatic water deficit ( $ET_{pot} >$  precipitation) from July to November, characterizing a distinct dry season which occasionally extends until February. The mean annual air temperature was approximately  $26.9 \pm 0.6^{\circ}\text{C}$  with maxima and minima of  $32.2 \pm 0.7^{\circ}\text{C}$  and  $23.4 \pm 0.6^{\circ}$ , respectively. Monthly maximum temperatures during the dry season were higher ( $32.0\text{--}33.5^{\circ}\text{C}$ ) than those of the rainy season ( $31.3\text{--}31.8^{\circ}\text{C}$ ). The hydrographic regime of the blackwater rivers (Negro, Unini, Jaú and Carabinani) in the study region was characterized by a monomodal flood pulse with maximum water levels peaking in the period end of June and beginning of July, while the minimum water levels occurred around October/November (Figure 3). The annual amplitude of the Negro River and the lower section of the Carabinani and Jaú rivers varied from 9.7 to 10.3 m. Upstream the rapids, the amplitude of the flood pulse declined and the hydro-regime became more irregular. Data from the Unini River upstream of the rapids indicates an annual amplitude of approximately 6.5 m with a more extended low-water period compared to the other analyzed river sections (Figure 3).

### Fire Occurrence in the Study Region

From 1982/1983 to 2016/2017, a total of 17,524 ha of burned floodplain forests have been mapped in the study region, distributed among 18 years and corresponding to 3.4% of the total studied *igapó* area. About 11,159 ha (63.7%) of burned *igapós* burned were located along the Unini River, 3,860 ha (22.0%) were identified along the Jaú River, 1,883 ha (10.7%) along the Negro River section and 628 ha (3.6%) along the Carabinani River (Figure 4). The majority of burned floodplain forest (61.5%) occurred in the buffer zone of the JNP, mainly along the Unini River and less extensively along the Negro River section. Interestingly, no fire scars were observed in the adjacent upland (*terra-firme*) forests during the 35-year study period. These fires comprised 254 fire scars, concentrated on the eastern and northern sections of the study region (Figure 4). The majority (78.7%) of the burnt areas was observed within a 10-km radius around human settlements, with 24.8% at 5–10 km, 24.8% at 2.5–5 km and 29.1% closer than 2.5 km distance. The detected fire scars were mainly concentrated in the size class of 4.1–40 ha (52.8%) (Table 1). Small-scale fires (<4.0 ha), large burnt areas (40.1–100 ha), and large-scale fires (>100 ha) shared 11.4, 15.7, and 20.1% of the fire scars, respectively. Large-scale fires accounted for 71.6% of the total burnt area of *igapó* in the



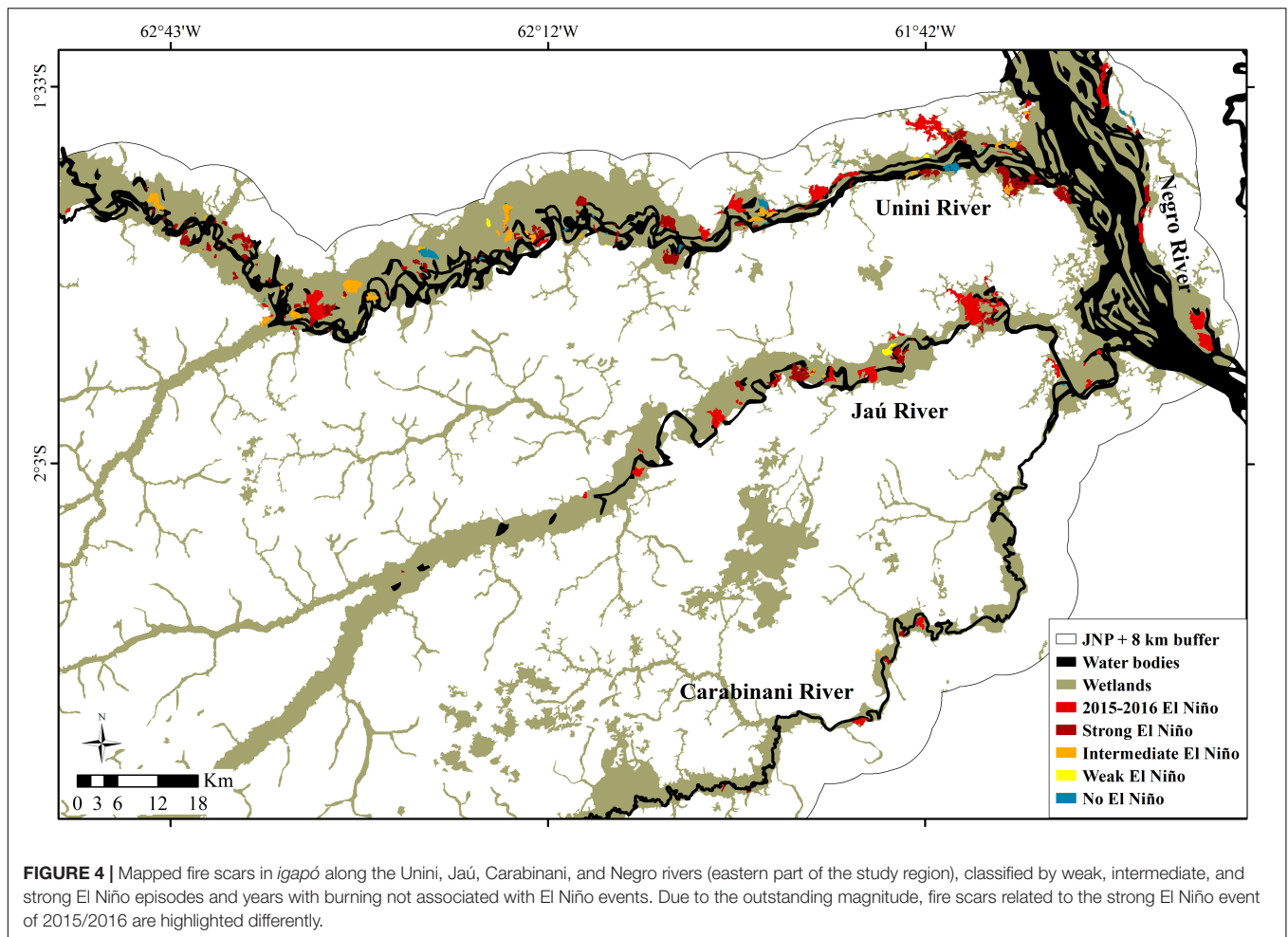
study region, while the size classes < 4.0, 4.1–40, and 40.1–100 ha shared 0.4, 12.1, and 15.9%, respectively. Although large-scale fires comprise only 20% of the total number of detected fire scars, they jointly represent over 70% of the total burnt area during the study period and occurred mainly during strong El Niño episodes.

From the 254 detected fires scars, 37 (14.6%) burnt at least twice during the monitored period, most of them in the *igapós* of the Unini ( $n = 29$ ) and to a less extent along the Jaú ( $n = 6$ ) and Negro ( $n = 2$ ) rivers. Recurring fires on the same area were observed twice (31 areas), three (5 areas) or even four times (1 area) during the monitored 35-year period with an average return period of  $13.2 \pm 8.5$  years. In general, the repeatedly occurring fires affected on average 57.0% of the original burnt area, however, with a huge variation (standard deviation of 40.7%). About 60% of the recurring fires occurred on areas < 10 ha and only 5% represented large-scale fires (> 100 ha). The burnt area by recurring fires accounted for 8.1% (1,412.4 ha) of the

total observed burnt area and was mainly concentrated along the Unini River (95.5%). Most recurring fires were observed during strong El Niño episodes such as during 1997/1998 (5 scars with 312.7 ha) and 2015/2016 (18 scars with a total area of 315.3 ha). However, also during years without El Niño conditions repeated fires were detected such as in 2001/2002 and 2003/2004 with a total burnt area of even 493.2 ha, all concentrated in *igapós* along the Unini River.

### Relationships Between Burnt *Igapó* Floodplains and Hydroclimatic Conditions

Significant trends of hydroclimatic parameters during the terrestrial phase (September to February) of the *igapó* floodplains were observed for  $T_{max}$  ( $Z = 3.81$ ,  $p < 0.001$ ) and a negative trend for  $MCWD$  ( $Z = -2.95$ ,  $p < 0.01$ ) along the 35 years (Figure 5). The remaining hydroclimatic parameters showed no significant



trends during the study period but a large interannual variation. The comparison of hydroclimatic conditions of the terrestrial phase between periods with and without fire occurrence indicated significant differences for all analyzed parameters ( $p < 0.05$ ) (Table 2). Periods with fire occurrence had, on average, an elevated  $T_{max}$  by  $0.9^{\circ}\text{C}$  during the terrestrial phase, while  $P$  and  $MCWD$  were reduced by 230 mm and 120 mm on average, respectively. The  $WL_{min90}$  was significantly lowered by 1.2 m, and  $BFI$  was decreased by 0.13 on average during periods with fire occurrence. Overall, the average  $ONI$  indicated for years with fire occurrence El Niño conditions ( $0.51 \pm 1.24^{\circ}\text{C}$ ), while for years without burning  $ONI$  was negative ( $-0.48 \pm 0.76^{\circ}\text{C}$ ).

During the studied period, fires in the *igapó* floodplain occurred mainly during El Niño events, which accounted for about 92.4% of the total burnt area in the *igapó* floodplains, while 7.6% of the burnt areas were attributed to eight further non-El Niño years (Table 1 and Figure 4). From the 12 El Niño episodes on record during the monitored period, only two events (1986/1987 and 2014/2015) were not related to *igapó* fires (Figure 5). Overall, El Niño affected mainly the climatic conditions in the study region leading to significantly increased  $T_{max}$ , while  $P$  and  $MCWD$  were significantly reduced (Table 2). Hydrological variables ( $WL_{min90}$  and  $BFI$ ) did not significantly differ between El Niño and other years. El Niño events of

intermediate ( $n = 4$ ) and weak intensities ( $n = 3$ ) contributed only to 9.4% and 1.5% of the total burnt *igapó* area, respectively. Hydroclimatic conditions during weak and intermediate El Niño intensities did not show significant differences compared to other years. The five El Niño episodes with strong intensities ( $ONI > 1.5^{\circ}\text{C}$ ; 1982/1983, 1991/1992, 1997/1998, 2009/2010, and 2015/2016) were of remarkable impact, corresponding to 81.5% of the total burnt area (Table 1). Hydroclimatic conditions of the terrestrial phase during strong El Niño events were characterized by elevated  $T_{max}$  ( $33.6 \pm 0.9^{\circ}\text{C}$ ) and extreme hydrometeorological droughts reflected by low  $P$  ( $742 \pm 171$  mm),  $MCWD$  ( $-389 \pm 180$  mm),  $WL_{min90}$  ( $148 \pm 77$  cm) and  $BFI$  ( $0.16 \pm 0.09$ ) (Table 2). These severe drought episodes comprise more than 80% of the large-scale fires ( $> 100$  ha). More than 7,506 ha (42.8%) of the total burnt *igapó* floodplain forests in the study region were associated with the strong El Niño 2015/2016 (Table 1). At the Jaú River, more than 2,428 ha *igapó* burnt during this period, corresponding to 62.9% of the total burnt area along this river. Also other river sections of the study area accounted in this period for the largest observed burnt areas with 67.5% (Carabinani River), 70.4% (Negro River) and 29.8% (Unini River), referring to the total of mapped burnt *igapó* during the study period (Figure 4). During this El Niño event, the highest  $T_{max}$  ( $34.8^{\circ}\text{C}$ ), and lowest values

**TABLE 1** | Mapped fire scars indicating their number (in brackets) and total area (in hectare) by size classes during periods with strong (ONI > 1.5°C), intermediate (ONI 1.0–1.5°C), and weak (ONI 0.5–1.0°C) El Niño events and years without El Niño occurrence.

|                        | Period       | ≤4.0 ha          | 4.1–40.0 ha          | 40.1–100.0 ha       | > 100 ha             | Total                 |
|------------------------|--------------|------------------|----------------------|---------------------|----------------------|-----------------------|
| Strong El Niño         | 1982/1983    | 7.7 (2)          | 211.5 (14)           | 210.9 (4)           | 1,196.0 (5)          | <b>1,621.1 (25)</b>   |
|                        | 1991/1992    | 9.0 (4)          | 408.4 (28)           | 730.4 (13)          | 1,546.5 (7)          | <b>2,694.3 (52)</b>   |
|                        | 1997/1998    | 15.8 (7)         | 226.9 (14)           | 592.1 (7)           | 985.1 (5)            | <b>1,820.0 (33)</b>   |
|                        | 2009/2010    | –                | 134.6 (7)            | 85.7 (1)            | 419.6 (2)            | <b>639.9 (10)</b>     |
|                        | 2015/2016    | 4.0 (2)          | 393.5 (23)           | 409.3 (6)           | 6,699.5 (22)         | <b>7,506.3 (53)</b>   |
|                        | <b>Total</b> | <b>36.5 (15)</b> | <b>1,374.9 (86)</b>  | <b>2,028.4 (31)</b> | <b>10,846.7 (41)</b> | <b>14,286.5 (173)</b> |
| Intermediate El Niño   | 1987/1988    | –                | 68.5 (4)             | –                   | –                    | <b>68.5 (4)</b>       |
|                        | 1994/1995    | 6.8 (3)          | 137.9 (9)            | 75.2 (1)            | 822.8 (4)            | <b>1,042.8 (17)</b>   |
|                        | 2002/2003    | 11.3 (5)         | 71.2 (7)             | 326.1 (4)           | 123.1 (1)            | <b>531.7 (17)</b>     |
|                        |              | <b>Total</b>     | <b>18.1 (8)</b>      | <b>277.6 (20)</b>   | <b>401.3 (5)</b>     | <b>945.9 (5)</b>      |
| Weak El Niño           | 2004/2005    | –                | 51.8 (2)             | –                   | 134.8 (1)            | <b>186.6 (3)</b>      |
|                        | 2006/2007    | –                | 25.7 (1)             | 46.3 (1)            | –                    | <b>72.0 (2)</b>       |
|                        |              | <b>Total</b>     | –                    | <b>77.5 (3)</b>     | <b>46.3 (1)</b>      | <b>134.8 (1)</b>      |
| Years without El Niños | 1985/1986    | –                | 8.3 (1)              | –                   | 265.3 (1)            | <b>273.6 (2)</b>      |
|                        | 1998/1999    | 3.3 (1)          | 97.1 (6)             | 53.4 (1)            | 128.9 (1)            | <b>282.7 (9)</b>      |
|                        | 2000/2001    | 5.2 (2)          | 5.5 (1)              | –                   | –                    | <b>10.7 (3)</b>       |
|                        | 2001/2002    | –                | 79.0 (5)             | 112.4 (2)           | 173.2 (1)            | <b>346.6 (8)</b>      |
|                        | 2003/2004    | –                | 121.7 (7)            | –                   | 193.4 (1)            | <b>315.6 (8)</b>      |
|                        | 2010/2011    | –                | 52.4 (3)             | –                   | –                    | <b>52.4 (3)</b>       |
|                        | 2011/2012    | –                | 25.8 (1)             | –                   | –                    | <b>25.8 (1)</b>       |
|                        | 2012/2013    | 4.5 (3)          | 6.0 (1)              | –                   | –                    | <b>10.5 (4)</b>       |
|                        | <b>Total</b> | <b>13.0 (6)</b>  | <b>395.8 (25)</b>    | <b>165.8 (3)</b>    | <b>761.3 (3)</b>     | <b>1,335.9 (38)</b>   |
| Study period           |              | <b>67.6 (29)</b> | <b>2,125.8 (134)</b> | <b>2,776.6 (40)</b> | <b>12,553.9 (51)</b> | <b>17,523.9 (254)</b> |

Bold values indicate total values of burnt area (fire scars) by size classes and periods.

for  $P$  (507 mm),  $MCWD$  (–635 mm),  $WL_{min90}$  (84 cm) and  $BFI$  (0.07) were observed for the terrestrial phase during the entire studied period (Figure 5). Hydroclimatic parameters explained a large portion of the annual burnt *igapó* forests in the study region as shown in Figure 6 by non-linear (exponential) regression models with adjusted  $R^2$  varying from 0.61 ( $WL_{min90}$ ) to 0.90 ( $MCWD$ ). The standard deviation of the residuals (observed–estimated burnt area) ranged from 846 ha ( $WL_{min90}$ ) to 436 ha ( $MCWD$ ).

During our remotely monitored period, the IPO experienced a warm phase until 1998 and since 2014, with a cold phase in-between (1999–2013) (Buckley et al., 2019). The strongest El Niño events on record (1982/1983, 1997/1998, and 2015/2016) coincided with warm phases of the IPO, resulting in significantly increased air temperature and severe hydrometeorological conditions during the terrestrial phase of the studied *igapó*. These three events alone accounted for 62.5% of the burnt *igapó* detected along the 35-year period. The years with burnt *igapó* forests exceeding 1,000 ha in the study region occurred all during El Niño events throughout warm IPO phases with strong (1982/1983, 1991/1992, 1997/1998, and 2015/2016) or intermediate (1994/1995) intensities.

## DISCUSSION

We show in this study that fires in the *igapó* occur mainly during severe hydroclimatic drought conditions associated with El Niño events (Table 1). El Niños generate increased air temperature,

reduced precipitation and increased  $MCWD$  (Figure 5) during the terrestrial phase of the floodplains which extend into the rainy season. The dry hydroclimatic conditions during the low-water period turn *igapó* forests vulnerable to understory fires as evidenced by previous studies (Nelson, 2001; Ritter et al., 2012; Santos and Nelson, 2013; Flores et al., 2014, 2016, 2017; Resende et al., 2014; Almeida et al., 2016; Flores and Holmgren, 2021). The outstanding dry hydroclimatic conditions in the studied *igapó* during the extreme drought in 2015/2016, induced by El Niño “Godzilla,” attributed almost 43% of the burnt *igapó* area during the entire study period. A series of severe and long-lasting flood events occurred during four consecutive years (2012–2015) in the lower Negro River basin (Barichivich et al., 2018; Schöngart and Junk, 2020) before this extreme event. These comparatively long-lasting anoxic conditions likely resulted in a surplus of litter accumulation, particularly at low topographic elevations (Carvalho, 2019). Possibly, the combined effect of litter accumulation during several consecutive years and the extreme drought conditions in 2015/2016 favored the widespread of fires in *igapós* affecting large areas.

Similar results were observed for *igapós* of the Mariuá Archipelago at the middle Negro River (Figure 1), close to the city of Barcelos (Flores et al., 2014). Using Landsat imagery, Flores and Holmgren (2021) analyzed a 40-year period of fire occurrences of *igapó* floodplains in the Mariuá Archipelago covering an area of 4,100 km<sup>2</sup>. Fires affecting *igapó* landscapes remained in total under 10,000 ha for the period 1973–2014 (Flores et al., 2014), but exceeded 70,000 ha during

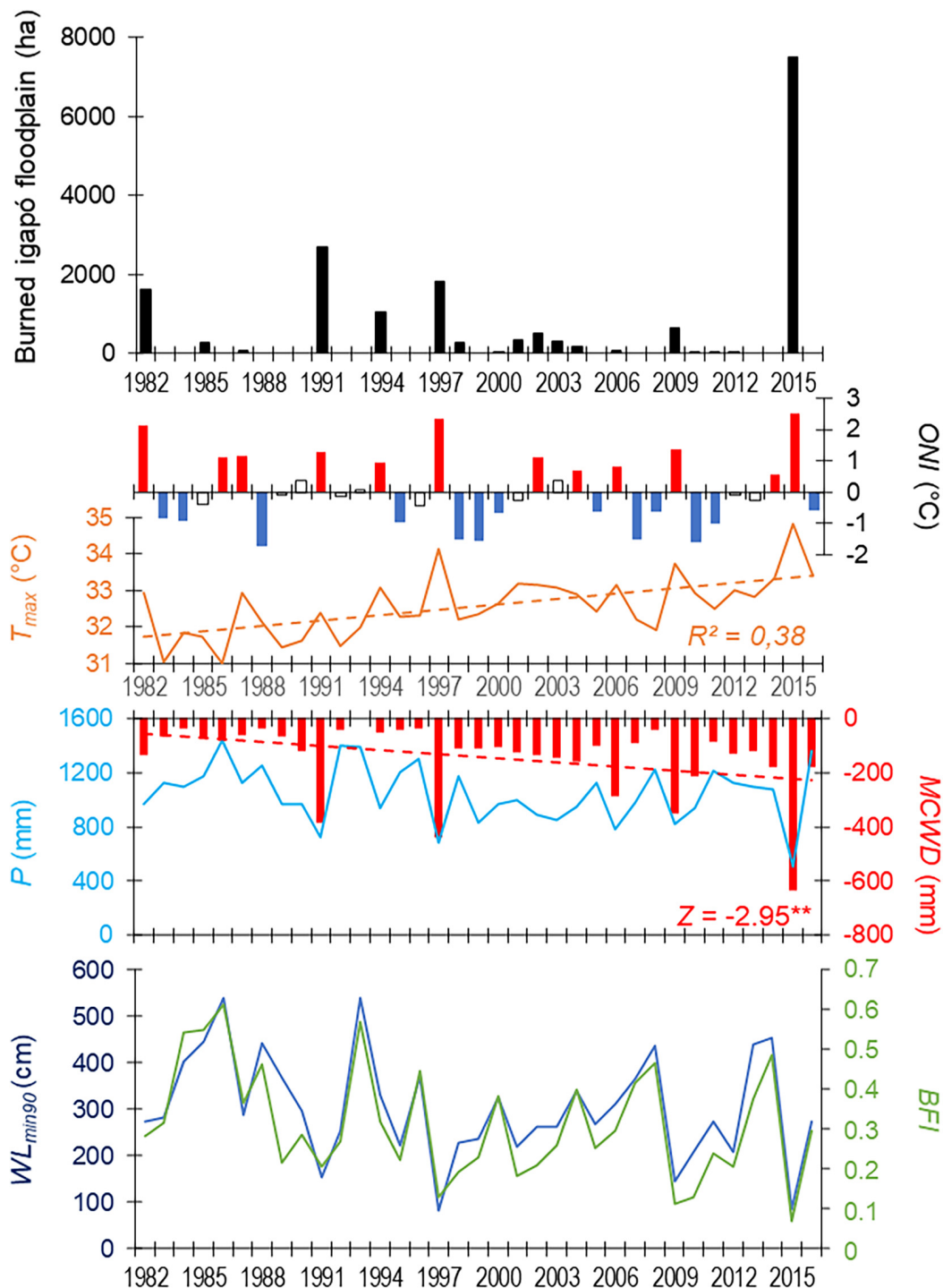


**FIGURE 5 |** Time series of burnt *igapó* forests, large-scale (Oceanic Niño Index—ONI; red bars indicate El Niño events and blue bars La Niña episodes) and regional climatic (monthly maximum temperature— $T_{max}$ , cumulative precipitation— $P$ , maximum cumulative water deficit— $MCWD$ ) and hydrological conditions (90-day minimum water level— $WL_{min90}$  and baseflow index— $BFI$ ) calculated for the terrestrial phase (September–February) of *igapó* floodplain forests. Dashed lines indicate significant trends of hydroclimatic variables along the 35-year study period (99.9% (\*\*\*) and 99.0% (\*\*)) confidence levels.

the severe hydrometeorological drought conditions during the strong El Niño 2015/2016 (Flores and Holmgren, 2021). While the amount and seasonality of rainfall in this region is similar

to that of our study site, the hydrographic conditions of the Mariuá Archipelago are different. Compared to the lower Negro River, the flood amplitude is only 5–6 m, and the low-water

**TABLE 2** | Differences of large-scale (ONI) and regional hydroclimatic conditions ( $T_{max}$ ,  $P$ ,  $MCWD$ ,  $WL_{min90}$ , and  $BFI$ ) between periods ( $n$ ) of fire occurrence and those without calculated for the terrestrial phase (September–February) of floodplain forests.

|                 | $n$ | ONI (°C)        | $T_{max}$ (mm) | $P$ (mm)    | MCWD (mm)  | $WL_{min90}$ (cm) | BFI         |
|-----------------|-----|-----------------|----------------|-------------|------------|-------------------|-------------|
| Fire occurrence | 18  | 0.51 ± 1.24     | 33.0 ± 0.7     | 936 ± 188   | −201 ± 158 | 247 ± 92          | 0.25 ± 0.12 |
| Without fires   | 17  | −0.48 ± 0.76    | 32.1 ± 0.7     | 1,166 ± 175 | −79 ± 51   | 346 ± 101         | 0.38 ± 0.13 |
| MW-test         |     | *               | ***            | **          | **         | **                | **          |
|                 | $n$ | Burnt area (ha) | $T_{max}$ (mm) | $P$ (mm)    | MCWD (mm)  | $WL_{min90}$ (cm) | BFI         |
| El Niños (EN)   | 12  | 1,349 ± 2,122   | 33.1 ± 0.9     | 909 ± 239   | −242 ± 180 | 272 ± 140         | 0.29 ± 0.16 |
| Other years     | 23  | 57 ± 117        | 32.3 ± 0.6     | 1,120 ± 162 | −90 ± 51   | 321 ± 94          | 0.33 ± 0.13 |
| MW-test         |     | ***             | **             | **          | **         | n.s.              | n.s.        |
| Strong EN       | 5   | 2,857 ± 2,699   | 33.6 ± 1.0     | 742 ± 171   | −389 ± 180 | 148 ± 77          | 0.16 ± 0.09 |
| Intermediate EN | 4   | 411 ± 483       | 32.6 ± 1.0     | 1,097 ± 248 | −82 ± 38   | 355 ± 126         | 0.38 ± 0.17 |
| Weak EN         | 3   | 86 ± 94         | 33.1 ± 0.2     | 937 ± 147   | −208 ± 69  | 368 ± 75          | 0.39 ± 0.09 |

Differences of burnt *igapó* forests and regional hydroclimatic conditions between El Niño (EN) episodes and other years. Indicated are mean values and standard deviations, also separated for strong (ONI > 1.5°C), intermediate (ONI 1.0–1.5°C) and weak (ONI 0.5–0.9°C) El Niño events. Differences were tested by a Mann-Whitney (MW) U Test; asterisks indicate the confidence levels of 99.9% (\*\*\*), 99% (\*\*), 95% (\*), and not significant (n.s.).

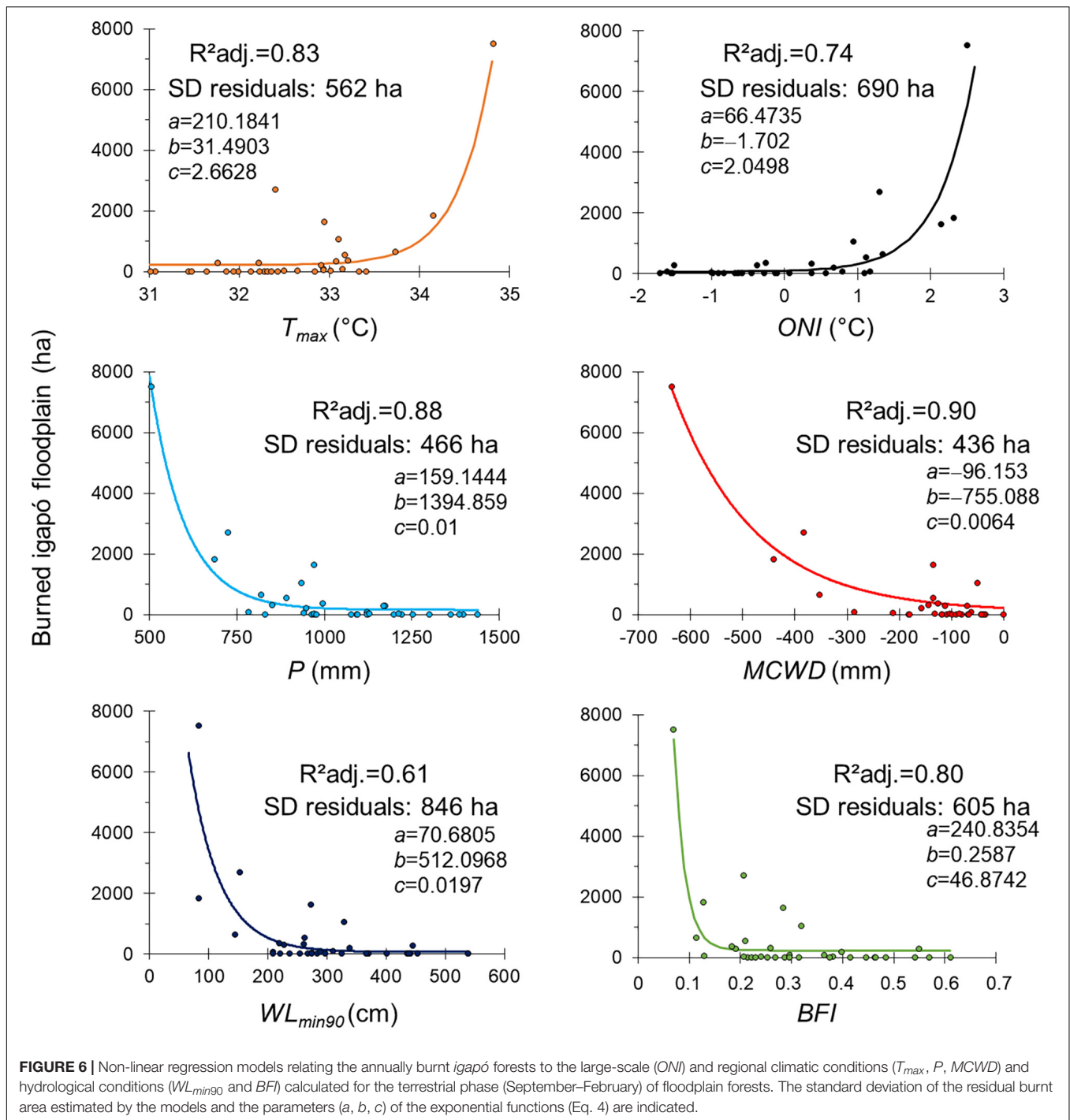
period occurs 3–4 months later, which temporarily expands the hydroclimatic drought conditions generated by El Niño. Considering that the *igapó* floodplains of the Mariuá Archipelago are not integrated in the framework of protected areas at the national level (Figure 1), and that hydroclimatic drought conditions persist for longer periods in this region due to the later occurrence of the low-water period possibly explain the higher percentage of burnt *igapós* in this region. Compared to our study site where about 3.4% of *igapó* floodplains were affected by fire without significant numbers of repeated fire occurrence, about 19.5% of the *igapó* floodplains in the Mariuá Archipelago burnt during a similar observation period, in which 48% of fire scars burnt at least twice (Flores and Holmgren, 2021). The percentage of fire scars which burnt at least twice is with 14.6% considerably lower in our study, especially when accounting for the total burnt area which represents only 8.1% of the total burnt area. Burnt areas need long periods to recover due to the slow dynamical processes in this ecosystem (Flores et al., 2014; Flores and Holmgren, 2021). The establishing open vegetation is susceptible to recurring fire events due to the dry microclimate, the occurrence of herbaceous species, and the accumulation of dead biomass (Flores et al., 2016).

## Fire Ignition in *Igapós*

Generally, the humid conditions of Amazonian rainforests do not allow for the propagation of wildfires caused by natural ignition, such as lightning, and human presence is the leading cause of fires in the Amazon basin (Bowman et al., 2011; Pivello, 2011). During recent decades increasing human pressure resulted in spatiotemporal increases of fire, mainly in Amazonian *terra-firme* (Aragão et al., 2018). *Igapós* in our study region, however, are seasonally flooded for several months, have a relatively low human population density (< 0.04 persons/km<sup>2</sup>; Pinheiro and Macedo, 2004), do not suffer significant impacts from land-use changes, and are mostly integrated in protected areas (Figure 1). Even though, large-scale fires are evident, especially during El Niño-induced severe droughts. The fire spots detected in this study do not follow a homogeneous pattern of spread and

frequency in *igapó* floodplains. About 79% of the mapped fire scars were detected in regions close to human settlements and communities (<10 km distance). This suggests that the origin of *igapó* fires is mainly caused by humans. More than 54% of the detected fire scars occurred close to human settlements (<5 km distance) suggesting that fires commonly applied during slash-and-burn activities in neighboring areas such as *terra-firme* forests, accidentally escape and are the main source of fire ignition in *igapó* forests. Most of the fires in *igapós* that occurred outside the community boundaries (>10 km radius) were located between settlements and communities, mainly along the lower section of the Unini River, destined for land-use (ICMBio, 2014). In this section we also observed most recurring fires events which generally occur at small-scales (<10 ha) and were detected also during non-El Niño conditions, suggesting anthropogenic ignition. Other common fire ignition sources in the *igapó* are not extinguished campfires on the river margins which might also occur at further distances to settlements (Ritter et al., 2012). Overall, fire ignition caused by humans in the study region seems to be accidental. Settlements of Pre-Columbian and modern populations until the late 1970s in northern Amazonia also showed a much higher amount of pyrogenic soil carbon in the region close to human occupation (< 3 km distance) than in more distant regions (Carvalho et al., 2018). These findings suggest that *igapós* in remote areas have a low probability of burning.

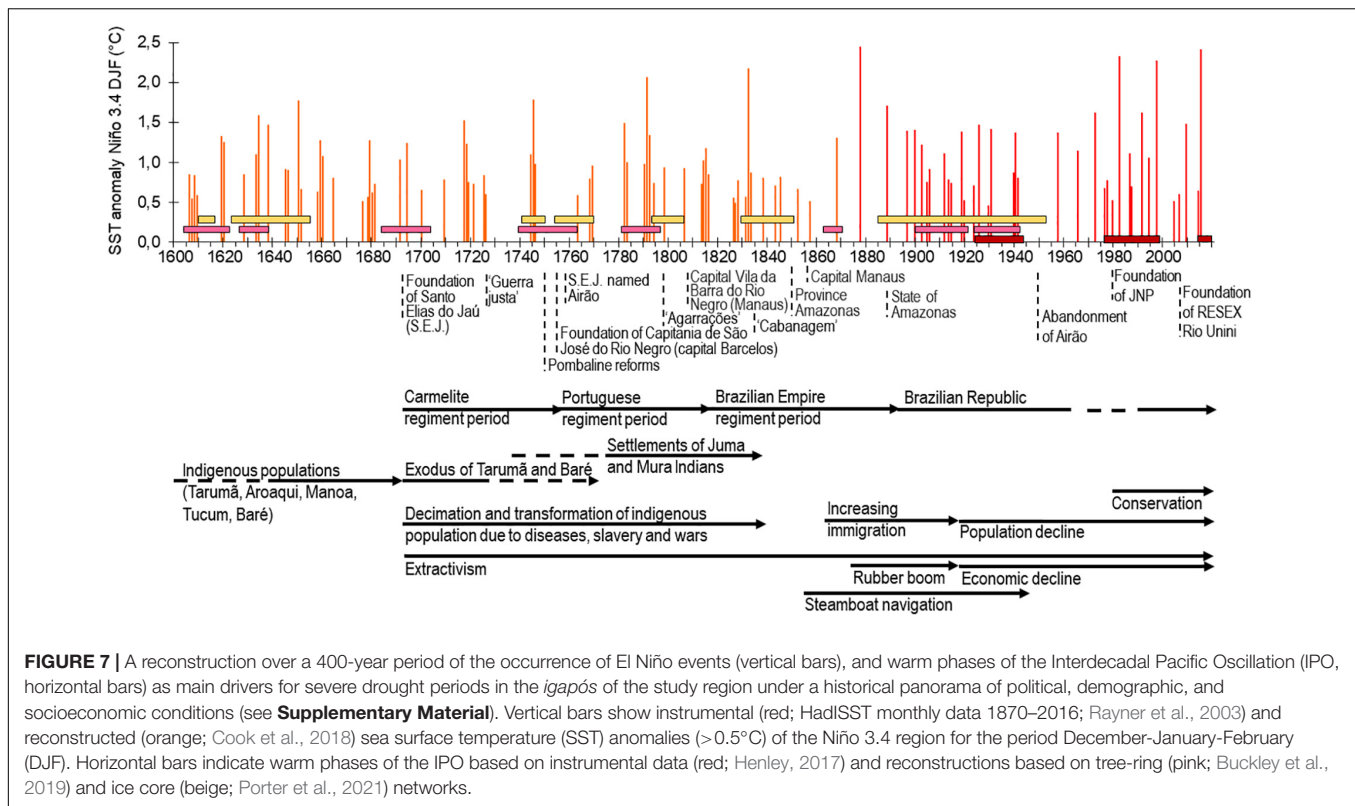
No fire scars have been detected during the analyzed 35-year period in the remote areas of the western part of the study region, lacking human settlements. An exception is the *igapó* along the Carabinani River. Although a small settlement exists in the lower section of the river downstream of the first rapid (Figure 2), the upstream areas with various rapids make access difficult and consequently reduce anthropogenic disturbance. However, some fire scars were also detected in the remote *igapós*. It might be possible that some of these fires were caused by natural events as observed by Moran (1990), such as frequent and intense lightning during the dry season in the study region (Christian et al., 2003). Amazonian floodplain trees represent



the largest known non-ebullitive emission of methane ( $CH_4$ ), produced under anaerobic conditions in the flooded soil mainly emitted by the trunk to the surface (Pangala et al., 2017). During field expeditions in *igapó* floodplains during the dry season, we frequently observed the enclosure of  $CH_4$  in large trunk hollows (see Video in **Supplementary Material**) when wood cores from large trees were extracted by increment borers. If these trees are hit by lightning, they may act as natural fire ignition source during a severe drought period.

## Historical Background of Past Disturbances in *Igapós* of the Study Region

We showed that fire disturbances in the *igapós* floodplains of the JNP and its surroundings occur mainly during severe El Niño events, especially during warm IPO phases, evidencing the role of human presence as the main source of fire ignition. Based on these findings we compile in **Figure 7** instrumental



(Rayner et al., 2003) and reconstructed El Niño events (Cook et al., 2018) for the last 400 years. Compared to the analyzed period, past climate conditions were characterized by plurianual El Niño episodes such as in 1606–1609, 1678–1681, 1717–1721, 1744–1746, 1790–1794, 1813–1816, 1826–1828, and 1831–1833 (**Figure 7**) suggesting that the study region was likely impacted by drought events with much stronger magnitudes and longer duration than any observed during instrumental periods (Parsons et al., 2018). We further argue that severe hydroclimatic droughts associated with El Niño events and large-scale fires in the *igapó* are intensified during warm IPO phases. Reconstructed warm IPO phases (Buckley et al., 2019; Porter et al., 2021) indicate congruence for the periods of 1610–1640, 1740–1765, at the end of the 18th century, and between 1900 and 1940. However, some periods, as 1680–1705 and during the 19th century, do not show temporal matches, probably because the proxies used for the reconstruction are related to different regions of the IPO (Buckley et al., 2019). The IPO reconstruction of Vance et al. (2015), based on a salt record from an Antarctic ice core, also suggests a warm phase for the period 1685–1720.

In the background of past El Niños and warm IPO phases, we highlight the historical background of the study region for the last 400 years (**Figure 7**), considering political, economic and sociocultural aspects mainly based on information from Leonardi (1999) (see **Supplementary Material** for more detailed information). We assume that the indigenous population inhabiting the study region before the arrival of the Portuguese colonizers made use of fire for small-scale agriculture or to develop ‘terra-preta’ soils (Bush et al., 2015). These anthropogenic

soils have a large amount of pyrogenic charcoal and occur in the study region adjacent to the rivers (Clement et al., 2015). Denevan (1996) suggests that most of the ancient human populations in Amazonia settled on areas adjacent to river floodplains, preventing the populations from periodic flooding and supporting them by multiple subsistence systems of a year-around agriculture in floodplains and adjacent *terra-firme* areas, hunting and fishing. Pre-Columbian pyrogenic carbon derived from soil charcoal is closely related to the distance of the next major river (Sanford et al., 1985; McMichael et al., 2012; Bush et al., 2015). Soil profiles from river banks of the nearby Anavilhanas Archipelago often present charcoal fragments, some associated with archeological artifacts and logs (Latrubesse and Franzinelli, 2005). These findings suggest that fires might have affected the *igapó* forests of the study region during the 17th century, especially during frequent and prolonged El Niño episodes of warm IPO phases. However, anthropologic studies indicate that indigenous populations of the Negro River had a cautious and controlled use of fire for agriculture purposes (Ribeiro, 1995).

The colonization of the study region, first by the Carmelite missionaries (1694–1750) and later by the Portuguese Empire regime resulted in increasing extraction of forest products in the study region during the 18th century. Likely sporadic fires occurred in the *igapós* during prolonged and intense El Niño conditions, especially when warm IPO phases predominated, such as during the 1790s. This period is well-known in other tropical regions, such as the Settlement Drought in Eastern Australia (1791–1792; Palmer et al., 2015), corresponding to

the East India Drought (1790–1796; Cook et al., 2010) and multiannual pluvials in subtropical regions of North (1791–1796) and South (1792/1793) America (Stahle et al., 2016; Morales et al., 2020), associated with the mega-El Niño in the period 1789–1793 (Grove, 2007). During the first half of the 19th century, the region suffered economic and demographic decay and heavy decimation of the indigenous and descendants, first by the Portuguese oppressors and later by the Brazilian Empire (Figure 7). Even if prolonged El Niño conditions occurred during the first half of the 19th century, the frequency and extension of fires in the *igapós* was probably reduced.

Since the creation of the Amazonas Province in 1850 with Manaus as capital (1856), this scenario changed profoundly. Steamboat navigation started in 1854 along the Negro River between Manaus and Sta. Isabel do Rio Negro and Airão became a strategic location to supply firewood for steamboats and harvests of *igapó* forests occurred in the lower Jaú River basin (Leonardi, 1999). The highest positive index in the IPO reconstruction based on tree rings is the year 1865 (Buckley et al., 2019), which is the driest year of a 250-year rainfall reconstruction in Eastern Amazonia within seven consecutive drought years (1864–1870) (Granato-Souza et al., 2019) associated with another short warm phase of the IPO, as suggested by Buckley et al. (2019). Another well-documented El Niño event occurred in 1877–1878, inducing severe drought hazards in many tropical regions, including the Amazon basin and the semi-arid Brazilian Northeast (Aceituno et al., 2009). The year 1878 appears as an outstanding positive IPO index in the 700-year reconstruction (Buckley et al., 2019) and is also evident in a tree ring-based reconstruction of teleconnections between El Niño and the hydrological regime at the middle Solimões River (Schöngart et al., 2004). These extreme drought events in a period of increasing harvest and human occupation in the study region likely caused frequent large-scale fires in *igapó* forests. After the strong El Niño episode in 1877–1878, which caused massive socioeconomic decay in the Brazilian Northeast, thousands of immigrants from these regions settled during the rubber boom distributed over a hundred locations in the lower sections of the Jaú, Carabinani and Unini rivers, but also upstream of the rapids, performing extraction of latex (*Hevea* spp.) and other forest products (Leonardi, 1999). This induced a profound sociocultural transformation of the study region. The use of fire in the predominantly savanna and semi-desert regions of Northeast Brazil is a common practice of these populations (Pivello, 2011), who had no intrinsic relationship with the humid tropical forests of the Amazon region (Leonardi, 1999). Intensified harvest occurred in *igapó* forests to extract firewood for the vulcanization of rubber and to sustain the intensifying steamboat navigation along the Negro River (Leonardi, 1999). Over the 40-year period of the rubber boom, frequent El Niño episodes occurred during predominant warm IPO phases as suggested from the reconstructed and instrumental data (Figure 7), also evident in the 200-year long floodplain tree-ring record (Schöngart et al., 2004). Strong hydroclimatic droughts induced by El Niño events occurred, for instance, in 1906 and 1916 (Marengo and Espinoza, 2016), leading to extreme low water levels of the lower Negro River (Schöngart and Junk, 2020). The strong El Niño event in the period of 1925/1926 already

took place during the collapse of the rubber boom, but induced extreme hydrological drought conditions over an entire year in the Negro River basin (Williams et al., 2005), reflected by the lowest maximum water level on record. Most of the *igapó* forests during this event were not flooded (Piedade et al., 2013) and large-scale fires occurred in the Negro River basin as reported by a Salesian bishop from Barcelos (Sternberg, 1987; Sombroek, 2001). During the period 1950–1970 we assume again a low frequency and magnitude of *igapó* fires due to the predominating cold IPO phase, low El Niño frequency, declining population density and socioeconomic decay in the study region.

Overall, the provided insights suggest that fire disturbances in the *igapó* floodplains is not a recent disturbance vector. During periods in which intense human occupation in the study region coincided with frequent El Niño events and warm IPO phases, *igapó* floodplains were subjected to severe and frequent fire disturbances. This holds true especially for the period of the rubber boom (1880–1920). On the other side, periods characterized with low frequency and magnitude of El Niño events, especially during cold IPO phases, with simultaneously decline of human occupation in the study region, suggest minor fire disturbances in the floodplain landscape.

## CONCLUSION

In this study we associate the magnitude and frequency of fire disturbances in mostly protected *igapó* floodplains with El Niño-induced hydroclimatic droughts and human occupation which accidentally are the main source of fire ignition. Insights from the historical background suggest that fire disturbances in the studied *igapó* probably were, at least during some periods, more severe and frequent in the past than during the last 35 years under study. Reasons for that are lacking protection status, higher human population densities, and exposition to much stronger magnitudes and longer duration of severe droughts. The historical panorama of climatic and socioeconomic conditions presented in Figure 7 is also applicable to other *igapó* regions in the Negro River basin, such as the middle section of the Negro River near the city of Barcelos, which was exposed to similar land-use intensity during the past centuries than the study site investigated here (Leonardi, 1999; Sampaio, 2003). This has strong implications for forest dynamics, management, and the conservation of this vulnerable ecosystem. For a long time, the landscape of oligotrophic blackwater *igapós* was interpreted as consisting of forest communities with slow dynamics and of centurial ages (Junk et al., 2015). Based on the analyzed period of recent fire occurrence and the drawn historical panorama, the findings of this study suggest that *igapó* landscapes in regions with historical human occupation are a patchwork of successional forest types that sporadically establish after large-scale fire disturbances caused by severe hydroclimatic droughts mainly driven by severe El Niño events, especially during warm IPO phases. However, also extended flooding periods associated to La Niña years and cold IPO phases seem to have influence on tree mortality, especially at the lowest topographies of *igapós* in the study region (Resende et al., 2020). The analysis of the

age structure of *igapó* forests by tree-ring analyses at the JNP (Corrêa, 2017) and other blackwater floodplain forests of Central Amazonia (Neves et al., 2019) revealed tree cohorts with mean ages varying from 61 to 113 years, which possibly established after major disturbances occurring during the frequent El Niño-induced hydroclimatic droughts that occurred during the rubber boom (1880–1920). However, further studies are necessary to evidence the occurrence of severe droughts and fires in the *igapó* floodplains during the past, combining radiocarbon dating of pyrogenic soil charcoal and tree-ring studies to analyze the age structure of *igapó* forests. In addition, the construction of tree-ring chronology networks bring insights of past hydroclimatic conditions of the study region, which can be cross-dated with the IPO reconstructions and contemporaneous hydroclimatic patterns evidenced by the droughts atlases from other tropical and subtropical regions with ENSO-teleconnections (Cook et al., 2010; Palmer et al., 2015; Stahle et al., 2016; Morales et al., 2020).

Compared to the unprotected *igapó* floodplains along the middle Negro River close to the city of Barcelos, where about 17% of the floodplains have been affected by fires only during the 2015/2016 El Niño episode (Flores and Holmgren, 2021), the overall impacts in the studied and mostly protected *igapó* over the 35 years are with 3.4% relatively small. Most of the fires verified in this study were associated with accidental anthropogenic ignition sources related to campfires or agricultural practices, which under the extreme and extended El Niño-induced drought conditions develop to understory fires spreading deep into the *igapó* forest. Tree species of the *igapó* are not adapted to fires, leading to massive losses of macrohabitats and biodiversity, ecosystem functions and environmental services, affecting food webs and at the end land and resource use by traditional human populations. To mitigate the impacts of anthropogenic fire disturbances, we suggest measures to improve the protection of this vulnerable ecosystem. *Igapó* forests should be completely excluded from intensive land use in the RESEX Rio Unini, not allowing the use of fires in general. In areas used for agriculture and settlements adjacent to *igapós*, mechanisms to avoid the escape of fire from slash-and-burn activities, could be the establishment of a buffer in the terra-firme, adjacent to the *igapó*. Especially during El Niño years, fires should be controlled or completely avoided. However, the use of fire is essential and an intrinsic component of traditional populations' culture inhabiting the remote areas of the Amazon basin. Campaigns of environmental education for residents could be an effective measure to mitigate socioenvironmental impacts of fires in the *igapó*. As the IPO shifted around 2014 into a warm phase, severe El Niño droughts can be expected for the forthcoming years, inducing severe meteorological and hydrological droughts. The evolution of El Niño events, especially strong episodes, is evident mostly at the begin of the second semester of the year (e.g., Dijkstra et al., 2019) and several models are applied for regularly updated seasonal ENSO forecasts in the equatorial Pacific Ocean<sup>3</sup>. This allows the development of an early warning system to avoid fires or at least mitigate their

impacts. Overall, the *igapós* of the lower Negro River are meanwhile integrated in a network of protected areas, many of them, however, destined to sustainable resource management, natural resource extraction, and/or ecotourism (Figure 1). The Mariuá Archipelago along the middle Negro River, although integrated in the Ramsar Site Rio Negro, still lacks protected areas at the national level, which are of utmost urgency for the conservation of the vulnerable *igapós* from further fire disturbances. However, in the background of increasing temperature, hydroclimatic extreme events and land-use changes in *igapós* (Barichivich et al., 2018; Marengo et al., 2018; Schöngart et al., 2021), the establishment of protected areas is nowadays not a sufficient measure unless efficient public policies based on scientific knowledge are developed. Such efforts integrate different governmental levels, non-governmental organizations, traditional and indigenous populations, and relevant stakeholder groups (for instance, tourist agencies) to prevent or at least mitigate fires in *igapós* to maintain their unique biodiversity and provided environmental services. This is of essential relevance in the Amazon basin undergoing an unprecedented transition driven by more and more increasing anthropogenic forces, approaching ecosystems to potential tipping points (Lovejoy and Nobre, 2018), which are uncertain for the Amazonian *igapó* and other wetlands. Increasing fire disturbances in a future warming climate, interacting with other disturbances caused by land-use changes (hydropower dams, mining, and selective logging, etc.) and increasing frequency and magnitude of hydroclimatic extreme events, could approach *igapós* even faster to this critical point.

## DATA AVAILABILITY STATEMENT

The original contributions presented in the study are included in the article/**Supplementary Material**, further inquiries can be directed to the corresponding author.

## AUTHOR CONTRIBUTIONS

TC, FW, and JS conceived the idea. TC, AR, and TS performed the analysis of remote sensing data. TC, JS, and AR analyzed data and produced the figures. JS wrote the manuscript. FW, MP, AR, and TS provided critical contributions. All authors made significant intellectual contributions to the manuscript and agreed to be accountable for the content of the work.

## FUNDING

This work was supported by CNPq/CAPES/FAPS/BC, NEWTON PROGRAM FUND; grant number: 441590/2016-0; CNPq/MCTI/CONFAP-FAPs/PELD; grant number: 441811/2020-5; INCT-ADAPTA (CNPq grant number: 465540/2014-7; FAPEAM grant number: 062.1187/2017). This study was financed in part by the Coordenação de Aperfeiçoamento de Pessoal de Nível Superior – Brasil

<sup>3</sup>[https://www.cpc.ncep.noaa.gov/products/analysis\\_monitoring/ens0\\_advisory/ensodisc.shtml](https://www.cpc.ncep.noaa.gov/products/analysis_monitoring/ens0_advisory/ensodisc.shtml)

(CAPES) – Finance Code 001 and by the Technical/Scientific Cooperation Agreement between INPA and the Max-Planck-Society. AR thanks CNPq and FAPESP for financial support (grant #2019/24049-5).

## ACKNOWLEDGMENTS

This study has been conducted in the framework of the Long-Term Ecological Research Program (PELD) coordinated by the Brazilian National Council for Scientific and Technological

Development (CNPq). We thank the Institute Chico Mendes for Conservation of Biodiversity (ICMBio) for support during the study period.

## SUPPLEMENTARY MATERIAL

The Supplementary Material for this article can be found online at: <https://www.frontiersin.org/articles/10.3389/ffgc.2021.755441/full#supplementary-material>

## REFERENCES

- Aceituno, P., Prieto, M. R., Solari, M. E., Martínez, A., Poveda, G., and Falvey, M. (2009). The 1877–1878 El Niño episode: associated impacts in South America. *Clim. Change* 92, 389–416. doi: 10.1007/s10584-008-9470-5
- Adis, J. A., Erwin, T. L., Battistola, L. D., and Ketelhut, S. M. (2010). “The importance of floodplain forests for animal biodiversity: beetles in canopies of floodplain and upland forests,” in *Amazonian Floodplain Forests. Ecophysiology, Biodiversity and Sustainable Management*, eds W. J. Junk, M. T. F. Piedade, F. Wittmann, J. Schöngart, and P. Parolin (Dordrecht: Springer), 313–328.
- Aguiar, D. P. P. (2015). *Influência dos Fatores Hidro-Eddáficos na Diversidade, Composição Florística e Estrutura da Comunidade Arbórea de Igapó no Parque Nacional do Jaú, Amazônia Central*. Master's thesis. Manaus: Instituto Nacional de Pesquisas da Amazônia.
- Ahn, K. H., and Merwade, V. (2014). Quantifying the relative impact of climate and human activities on streamflow. *J. Hydrol.* 515, 257–266. doi: 10.1016/j.jhydrol.2014.04.062
- Alencar, A. A., Brando, P. M., Asner, G. P., and Putz, F. E. (2015). Landscape fragmentation, severe drought, and the new Amazon forest fire regime. *Ecol. Appl.* 25, 1496–1505. doi: 10.1890/14-1528.1
- Almeida, D. R. A., Nelson, B. W., Schiatti, J., Gorgens, E. B., Resende, A. F., Stark, S. C., et al. (2016). Contrasting fire damage and fire susceptibility between seasonally flooded forest and upland forest in the Central Amazon using portable profiling LiDAR. *Remote Sens. Environ.* 184, 153–160. doi: 10.1016/j.rse.2016.06.017
- Alvarado, S. T., Fornazari, T., Cóstola, A., Morellato, L. P. C., and Silva, T. S. F. (2017). Drivers of fire occurrence in a mountainous Brazilian cerrado savanna: tracking long-term fire regimes using remote sensing. *Ecol. Indic.* 78, 270–281. doi: 10.1016/j.ecolind.2017.02.037
- Anderson, L. O., Ribeiro Neto, G., Cunha, A. P., Fonseca, M. G., Mendes de Moura, Y., Dalagnol, R., et al. (2018). Vulnerability of Amazonian forests to repeated droughts. *Philos. Trans. R. Soc. B* 373:20170411. doi: 10.1098/rstb.2017.0411
- Andreoli, R. V., and Kayano, M. T. (2005). ENSO-related rainfall anomalies in South America and associated circulation features during warm and cold Pacific decadal oscillation regimes. *Int. J. Climatol.* 25, 2017–2030. doi: 10.1002/joc.1222
- Aragão, L. E. O. C., Anderson, L. O., Fonseca, M. G., Rosan, T. M., Vedovato, L. B., Wagner, F. H., et al. (2018). 21st century drought-related fires counteract the decline of Amazon deforestation carbon emissions. *Nat. Commun.* 9:536. doi: 10.1038/s41467-017-02771-y
- Aragão, L. E. O. C., Malhi, Y., Roman-Cuesta, R. M., Saatchi, S., Anderson, L. O., and Shimabukuro, Y. E. (2007). Spatial patterns and fire response of recent Amazonian droughts. *Geophys. Res. Lett.* 34:L07701.
- Baker, J. C. A., Garcia-Carreras, L., Gloor, M., Marsham, J. H., Buermann, W., da Rocha, H. R., et al. (2021). Evapotranspiration in the Amazon: spatial patterns, seasonality, and recent trends in observations, reanalysis, and climate models. *Hydrol. Earth Syst. Sci.* 25, 2279–2300. doi: 10.5194/hess-25-2279-2021
- Barichivich, J., Gloor, E., Peylin, P., Brienen, R. J. W., Schöngart, J., Espinoza, J. C., et al. (2018). Recent intensification of Amazon flooding extremes driven by strengthened Walker circulation. *Sci. Adv.* 4:eaat8785. doi: 10.1126/sciadv.aat8785
- Barlow, J., Berenguer, E., Carmenta, R., and França, F. (2020). Clarifying Amazonia's burning crisis. *Glob. Change Biol.* 26, 319–321. doi: 10.1111/gcb.14872
- Bivand, R., Keitt, T., Rowlingson, B., Pebesma, E., Sumner, M., Hijmans, R., et al. (2014). *Package 'rgdal'. R Package*.
- Borges, S. H., Cohn-Haft, M., Carvalhaes, A. M. P., Henriques, L. M., Pacheco, J. F., and Whittaker, A. (2001). Birds of Jaú National Park, Brazilian Amazon: species check-list, biogeography and conservation. *Ornitol. Neotrop.* 12, 109–140.
- Bowman, D. M. J. S., Balch, J., Artaxo, P., Bond, W. J., Cochrane, M. A., D'Antonio, C. M., et al. (2011). The human dimension of fire regimes on Earth. *J. Biogeogr.* 18, 2223–2236. doi: 10.1111/j.1365-2699.2011.02595.x
- Brando, P., Macedo, M., Silvério, D., Rattis, L., Paolucci, L., Alencar, A., et al. (2020). Amazon wildfires: scenes from a foreseeable disaster. *Flora* 268:151609. doi: 10.1016/j.flora.2020.151609
- Buckley, B. M., Ummenhofer, C. C., D'Arrigo, R. D., Hansen, K. G., Truong, L. H., Le, C. N. et al. (2019). Interdecadal Pacific Oscillation reconstructed from trans-Pacific tree rings: 1350–2004 CE. *Clim. Dyn.* 53, 3181–3196. doi: 10.1007/s00382-019-04694-4
- Bush, M. B., McMichael, C. H., Piperno, D. R., Silman, M. R., Barlow, J., Peres, C. A., et al. (2015). Anthropogenic influence on Amazonian forests in pre-history: an ecological perspective. *J. Biogeogr.* 42, 2277–2288. doi: 10.1111/jbi.12638
- Camposano, L., Robaina, L., and Samaniego, E. (2020). The Pacific decadal oscillation modulates the relation of ENSO with the rainfall variability in coast of Ecuador. *Int. J. Climatol.* 40, 5801–5812. doi: 10.1002/joc.6525
- Carvalho, L. C. S., Fearnside, P. M., Nascimento, M. T., and Barbosa, R. I. (2018). Amazon soil charcoal: pyrogenic carbon stock depends of ignition source distance and forest type in Roraima, Brazil. *Glob. Change Biol.* 24, 4122–4130. doi: 10.1111/gcb.14277
- Carvalho, T. C. (2019). *Susceptibilidade ao Fogo de Florestas de Igapó de Águas Pretas no Parque Nacional do Jaú, Amazônia Central*. Master's thesis. Manaus: Instituto Nacional de Pesquisas da Amazônia.
- Christian, H. J., Blakeslee, R. J., Boccippio, D. J., Boeck, W. L., Buechler, D. E., Driscoll, K. T., et al. (2003). Global frequency and distribution of lightning as observed from space by the Optical Transient Detector. *J. Geophys. Res. Atmos.* 108:4005. doi: 10.1029/2002JD002347
- Clement, C. R., Denevan, W. M., Heckenberger, M. J., Junqueira, A. B., Neves, E. G., Teixeira, W. G., et al. (2015). The domestication of Amazonia before European conquest. *Proc. R. Soc. B* 282:20150813. doi: 10.1098/rspb.2015.0813
- Cochrane, M. A. (2003). Fire science for rainforests. *Nature* 421, 913–919. doi: 10.1038/nature01437
- Cook, B. I., Williams, A. P., Smerdon, J. E., Palmer, J. G., Cook, E. R., Stahle, D. W., et al. (2018). Cold tropical Pacific sea surface temperatures during the late sixteenth-century North American megadrought. *J. Geophys. Res. Atmos.* 123, 11307–11320. doi: 10.1029/2018JD029323
- Cook, E. R., Seager, R., Heim, R. R. Jr., Vose, R. S., Herweijer, C., and Woodhouse, C. (2010). Megadroughts in North America: placing IPCC projections of hydroclimatic change in a long-term palaeoclimate context. *J. Quat. Sci.* 25, 48–61. doi: 10.1002/jqs.1303
- Corrêa, J. B. (2017). *Variação Espaço-Temporal do Estoque e Sequestro de Carbono na Biomassa Lenhosa ao Longo de um Gradiente Hidroedáfico em Florestas*

- Alagáveis de Igapó no Parque Nacional do Jaú, Amazônia Central. Master's thesis. Manaus: Instituto Nacional de Pesquisas da Amazônia.
- Davidson, E. A., Araújo, A. C., Artaxo, P., Balch, J. K., Brown, I. F., Bustamante, M. C. M., et al. (2012). The Amazon basin in transition. *Nature* 481, 321–328. doi: 10.1038/nature10717
- De Simone, O., Haase, K., Müller, E., Junk, W. J., Gonsior, G. A., and Schmidt, W. (2002). Impact of root morphology on metabolism and oxygen distribution in roots and rhizosphere from two Central Amazon floodplain tree species. *Funct. Plant Biol.* 29, 1025–1035. doi: 10.1071/PP01239
- Denevan, W. M. (1996). A bluff model of riverine settlement in prehistoric Amazonia. *Ann. Assoc. Am. Geogr.* 86, 654–681. doi: 10.1111/j.1467-8306.1996.tb01771.x
- Dijkstra, H. A., Petersik, P., Hernández-García, E., and López, C. (2019). The application of machine learning techniques to improve El Niño prediction skill. *Front. Phys.* 7:153. doi: 10.3389/fphy.2019.00153
- Flores, B. M., Fagoaga, R., Nelson, B. W., and Holmgren, M. (2016). Repeated fires trap Amazonian blackwater floodplains in an open vegetation state. *J. Appl. Ecol.* 53, 1597–1603. doi: 10.1111/1365-2664.12687
- Flores, B. M., and Holmgren, M. (2021). White-sand savannas expand at the core of the Amazon after forest wildfires. *Ecosystems*. 24, 1624–1637. doi: 10.1007/s10021-021-00607-x
- Flores, B. M., Holmgren, M., Xu, C., van Nes, E. H., Jakovac, C. C., Mesquita, R. C. G., et al. (2017). Floodplains as an Achilles' heel of Amazonian forest resilience. *Proc. Natl. Acad. Sci. U.S.A.* 114, 4442–4446. doi: 10.1073/pnas.1617988114
- Flores, B. M., Piedade, M. T. F., and Nelson, B. W. (2014). Fire disturbance in Amazonian blackwater floodplain forests. *Plant Ecol. Divers.* 7, 319–327. doi: 10.1080/17550874.2012.716086
- Furch, K., and Junk, W. J. (1997). "Physiochemical conditions in floodplains," in *The Central Amazon Floodplain: Ecology of a Pulsing System*, ed. W. J. Junk (Berlin: Springer Verlag), 69–108.
- FVA (1998). *Plano de Manejo do Parque Nacional do Jaú*. Manaus: Fundação Vitória Amazônica/IBAMA.
- Gloor, M., Barichivich, J., Ziv, G., Brienen, R., Schöngart, J., Peylin, P., et al. (2015). Recent Amazon climate as background for possible ongoing and future changes of Amazon humid forests. *Glob. Biogeochem. Cycles* 29, 1384–1399. doi: 10.1002/2014GB005080
- Granato-Souza, D., Stahle, D. W., Barbosa, A. C., Feng, S., Torbenson, M. C. A., Pereira, G. A., et al. (2019). Tree rings and rainfall in the equatorial Amazon. *Clim. Dyn.* 52, 1857–1869. doi: 10.1007/s00382-018-4227-y
- Granato-Souza, D., Stahle, D. W., Torbenson, M. C. A., Howard, I. M., Barbosa, A. C., Feng, S., et al. (2020). Multidecadal changes in wet season precipitation totals over the Eastern Amazon. *Geophys. Res. Lett.* 47:e2020GL087478. doi: 10.1029/2020GL087478
- Grove, R. H. (2007). The great El Niño of 1789–93 and its global consequences. *J. Mediev. Hist.* 10, 75–98. doi: 10.1177/097194580701000203
- Haase, K., and Rättsch, G. (2010). "The morphology and anatomy of tree roots and their aeration strategies," in *Amazonian Floodplain Forests. Ecological Studies (Analysis and Synthesis)*, eds W. J. Junk, M. T. F. Piedade, F. Wittmann, J. Schöngart, and P. Parolin (Dordrecht: Springer), 141–161.
- Haugaasen, T., and Peres, C. A. (2005). Tree phenology in adjacent Amazonian flooded and unflooded forests. *Biotropica* 37, 620–630. doi: 10.1111/j.1744-7429.2005.00079.x
- Heckenberger, M. J., Russell, J. C., Fausto, C., Toney, J. R., Schmidt, M. J., Pereira, E., et al. (2008). Pre-Columbian urbanism, anthropogenic landscapes and the future of the Amazon. *Science* 321, 1214–1217. doi: 10.1126/science.1159769
- Henley, B. J. (2017). Pacific decadal climate variability: indices, patterns and tropical-extratropical interactions. *Glob. Planet. Change* 155, 42–55. doi: 10.1016/j.gloplacha.2017.06.004
- Hess, L. L., Melack, J. M., Affonso, A. G., Barbosa, C., Gastil-Buhl, M., and Novo, E. M. L. M. (2015). Wetlands of the lowland Amazon basin: extent, vegetative cover, and dual-season inundated area as mapped with JERS-1 synthetic aperture radar. *Wetlands* 35, 745–756. doi: 10.1007/s13157-015-0666-y
- Hijmans, R. J., and van Etten, J. (2013). *Package 'raster'. R Package*.
- Householder, J. E., Schöngart, J., Piedade, M. T. F., Junk, W. J., ter Steege, H., Montero, J. C., et al. (2021). Modeling the ecological responses of tree species to the flood pulse of the Amazon Negro river floodplains. *Front. Ecol. Evol.* 9:628606. doi: 10.3389/fevo.2021.628606
- Huang, B., Thorne, P. W., Banzon, V. F., Chepurin, G., Lawrimore, J. H., Menne, M. J., et al. (2017). Extended reconstructed sea surface temperature version 5 (ERSSTv5), upgrades, validations, and intercomparisons. *J. Clim.* 30, 8179–8205. doi: 10.1175/JCLI-D-16-0836.1
- Hughes, M. K. (1971). Seasonal calorific values from a deciduous woodland in England. *Ecology* 52, 923–926. doi: 10.2307/1936045
- ICMBio (2014). *Plano de Manejo Participativo da Reserva Extrativista do Rio Unini, Amazonas, Brasil*. Novo Airão: Instituto Chico Mendes de Conservação da Biodiversidade.
- Irmiler, U., and Furch, K. (1980). Weight, energy and nutrient changes during decomposition of leaves in the emersion phase of Central-Amaozonia inundation forests. *Pedobiologia* 20, 118–130.
- Junk, W. J. (1989). "Flood tolerance and tree distribution in Central Amazonian floodplains," in *Tropical Forests: Botanical Dynamics, Speciation and Diversity*, eds L. B. Holm-Nielsen, I. C. Nielsen, and H. Balslev (New York, NY: Academic Press), 47–64.
- Junk, W. J., Bayley, P. B., and Sparks, R. E. (1989). "The Flood pulse concept in river-floodplain systems," in *Proceedings of the International Large River Symposium*, Vol. 106. (Ottawa, ON: Canadian Special Publication of Fisheries and Aquatic Sciences), 110–127.
- Junk, W. J., Piedade, M. T. F., Schöngart, J., Cohn-Haft, M., Adeney, J. M., and Wittmann, F. (2011). A classification of major naturally-occurring Amazonian lowland wetlands. *Wetlands* 31, 623–640. doi: 10.1007/s13157-011-0190-7
- Junk, W. J., Wittmann, F., Schongart, J., and Piedade, M. T. F. (2015). A classification of the major habitats of Amazonian black-water river floodplains and a comparison with their white-water counterparts. *Wetl. Ecol. Manage.* 23, 677–693. doi: 10.1007/s11273-015-9412-8
- Kauffman, J. B., Uhl, C., and Cummings, D. L. (1988). Fire in the Venezuelan Amazon. 1. Fuel biomass and fire chemistry in the evergreen rainforest of Venezuela. *Oikos* 53, 167–175. doi: 10.2307/3566059
- Labat, D., Espinoza, J.-C., Ronchail, J., Cochonneau, G., de Oliveira, E., Doudou, J. C., et al. (2012). Fluctuations in the monthly discharge of Guyana Shield rivers, related to Pacific and Atlantic climate variability. *Hydrol. Sci. J.* 57, 1081–1091. doi: 10.1080/02626667.2012.695074
- Latrubesse, E. M., and Franzinelli, E. (2005). The late quaternary evolution of the Negro River, Amazon, Brazil: implications for island and floodplain formation in large anabranching tropical systems. *Geomorphology* 70, 372–397. doi: 10.1016/j.geomorph.2005.02.014
- Latrubesse, E. M., and Stevaux, J. C. (2015). "The Anavilhanas and Mariuá archipelagos: fluvial wonders from the Negro River, Amazon basin," in *Landscapes and Landforms of Brazil*, eds B. Vieira, A. Salgado, and L. Santos (Dordrecht: Springer), 157–169.
- Leonardi, V. (1999). *Os Historiadores e os Rios; Natureza e Ruína na Amazônia Brasileira*. Brasília: Paralelo15/Editora da Universidade de Brasília.
- Lobo, G. S., Wittmann, F., and Piedade, M. T. F. (2019). Response of black-water floodplain (igapó) forests to flood pulse regulation in a dammed Amazonian river. *For. Ecol. Manage.* 434, 110–118. doi: 10.1016/j.foreco.2018.12.001
- Lovejoy, T. E., and Nobre, C. A. (2018). Amazon tipping point. *Sci. Adv.* 4:eaat2340. doi: 10.1126/sciadv.aat2340
- Marengo, J. A. (2004). Interdecadal variability and trends of rainfall across the Amazon basin. *Theor. Appl. Climatol.* 78, 79–96. doi: 10.1007/s00704-004-0045-8
- Marengo, J. A. (2009). Long-term trends and cycles in the hydrometeorology of the Amazon basin since the late 1920s. *Hydrol. Process.* 23, 3236–3244. doi: 10.1002/hyp.7396
- Marengo, J. A., and Espinoza, J. C. (2016). Extreme seasonal droughts and floods in Amazonia: causes, trends and impacts. *Int. J. Climatol.* 36, 1033–1050. doi: 10.1002/joc.4420
- Marengo, J. A., Souza, C. A. Jr., Thonicke, K., Burton, C., Halladay, K., Betts, R. A., et al. (2018). Changes in climate and land use over the Amazon region: current and future variability and trends. *Front. Earth Sci.* 6:228. doi: 10.3389/feart.2018.00228
- McMichael, C. H., Bush, M. B., Piperno, D. R., Silman, M. R., Zimmerman, A. R., and Anderson, C. (2012). Spatial and temporal scales of pre-Columbian disturbance associated with western Amazonian lakes. *Holocene* 22, 131–141. doi: 10.1177/0959683611414932

- Meade, R. H., Rayol, J. M., Da Conceicao, S. C., and Natividade, J. R. G. (1991). Backwater effects in the Amazon River basin of Brazil. *Environ. Geol. Water Sci.* 18, 105–114. doi: 10.1007/BF01704664
- Meyer, U., Junk, W. J., and Linck, C. (2010). “Fine root systems and mycorrhizal associations in two Central Amazonian inundation forests: igapó and várzea,” in *Amazonian Floodplain Forests. Ecological Studies (Analysis and Synthesis)*, eds W. J. Junk, M. T. F. Piedade, F. Wittmann, J. Schöngart, and P. Parolin (Dordrecht: Springer), 163–178.
- Montero, J. C., Piedade, M. T. F., and Wittmann, F. (2014). Floristic variation across 600 km of inundation forests (Igapó) along the Negro River, central Amazonia. *Hydrobiologia* 729, 229–246. doi: 10.1007/s10750-012-1381-9
- Morales, M. S., Cook, E. R., Barichivich, J., Christie, D. A., Villalba, R., LeQuesne, C., et al. (2020). Six hundred years of South American tree rings reveal an increase in severe hydroclimatic events since mid-20th century. *Proc. Natl. Acad. Sci. U.S.A.* 117, 16816–16823. doi: 10.1073/pnas.2002411117
- Moran, E. F. (1990). *A Ecologia Humana das Populações da Amazônia*. Petrópolis: Vozes.
- Nelson, B. W. (2001). “Fogo em florestas da Amazônia Central em 1997,” in *Proceedings of the 10th Brazilian Remote Sensing Symposium*, Foz do Iguaçu, 1675–1682.
- Nepstad, D., Schwartzman, S., Bamberger, B., Santilli, M., Ray, D., Schlesinger, P., et al. (2006). Inhibition of Amazon deforestation and fire by parks and indigenous lands. *Conserv. Biol.* 20, 65–73. doi: 10.1111/j.1523-1739.2006.00351.x
- Nepstad, D. C., Lefebvre, P. A., Silva, U. L., Tomasella, J., Schlesinger, P., Solorzano, L., et al. (2004). Amazon drought and its implications for forest flammability and tree growth: a basin-wide analysis. *Glob. Change Biol.* 10, 704–717. doi: 10.1111/j.1529-8817.2003.00772.x
- Neves, J. R. D., Piedade, M. T. F., Resende, A. F., Feitosa, Y. O., and Schöngart, J. (2019). Impact of climatic and hydrological disturbances on black-water floodplain forests in Central Amazonia. *Biotropica* 51, 484–489. doi: 10.1111/btp.12667
- Nguyen, P.-L., Min, S.-K., and Kim, Y.-H. (2021). Combined impacts of the El Niño–Southern oscillation and Pacific decadal oscillation on global droughts assessed using the standardized precipitation evapotranspiration index. *Int. J. Climatol.* 41, E1645–E1662. doi: 10.1002/joc.6796
- Nobre, C. A., Sampaio, G., Borma, L. S., Castilla-Rubio, J. C., Silva, J. S., and Cardoso, M. (2016). Land-use and climate change risks in the Amazon and the need of a novel sustainable development paradigm. *Proc. Natl. Acad. Sci. U.S.A.* 113, 10759–10768. doi: 10.1073/pnas.1605516113
- Palmer, J. G., Cook, E. R., Turney, C. S. M., Allen, K., Fenwick, P., Cook, B. I., et al. (2015). Drought variability in the eastern Australia and New Zealand summer drought atlas (ANZDA, CE 1500–2012) modulated by the interdecadal Pacific oscillation. *Environ. Res. Lett.* 10:124002. doi: 10.1088/1748-9326/10/12/124002
- Pangala, S., Enrich-Prast, A., Basso, L., Peixoto, R. B., Bastviken, D., Hornibrook, E. R. C., et al. (2017). Large emissions from floodplain trees close the Amazon methane budget. *Nature* 552, 230–234. doi: 10.1038/nature24639
- Parolin, P., De Simone, O., Haase, K., Waldhoff, D., Rottenberger, S., Kuhn, U., et al. (2004). Central Amazon floodplain forests: tree survival in a pulsing system. *Bot. Rev.* 70, 357–380.
- Parolin, P., Wittmann, F., and Schöngart, J. (2010). “Tree phenology in Amazonian floodplain forests,” in *Amazonian Floodplain Forests. Ecological Studies (Analysis and Synthesis)*, eds W. J. Junk, M. T. F. Piedade, F. Wittmann, J. Schöngart, and P. Parolin (Dordrecht: Springer), 105–126.
- Parsons, L. A., LeRoy, S., Overpeck, J. T., Bush, M., Cárdenes-Sandí, G. M., and Saleska, S. (2018). The threat of multi-year drought in Western Amazonia. *Water Resour. Res.* 54, 5890–5904. doi: 10.1029/2017WR021788
- Piedade, M. T. F., Ferreira, C. S., Oliveira Wittmann, A., Buckeride, M., and Parolin, P. (2010). “Biochemistry of Amazonian floodplain trees,” in *Amazonian Floodplain Forests. Ecological Studies (Analysis and Synthesis)*, eds W. J. Junk, M. T. F. Piedade, F. Wittmann, J. Schöngart, and P. Parolin (Dordrecht: Springer), 127–140.
- Piedade, M. T. F., Schöngart, J., Wittmann, F., Parolin, P., and Junk, W. J. (2013). “Impactos ecológicos da inundação e seca a vegetação das áreas alagáveis amazônicas,” in *Eventos Climáticos Extremos na Amazônia: Causas e Consequências*, eds C. A. Nobre and L. S. Borma (São Paulo: Oficina de Textos), 268–305.
- Pinheiro, M. R., and Macedo, A. B. (2004). “Dinâmica da população humana nos rios do Parque Nacional do Jaú,” in *Janelas para a Biodiversidade no Parque Nacional do Jaú: Uma Estratégia para o Estudo da Biodiversidade na Amazônia*, eds S. H. Borges, S. Iwanaga, C. C. Durigan, and M. R. Pinheiro (Manaus: Fundação Vitória Amazônica), 43–61.
- Pivello, V. R. (2011). The use of fire in the Cerrado and Amazonian rainforests of Brazil: past and present. *Fire Ecol.* 7, 24–39. doi: 10.4996/fireecology.0701024
- Pohlert, T. (2020). *Trend: Non-Parametric Trend Tests and Change-Point Detection. R Package Version 1.1.4*. Available online at: <https://CRAN.R-project.org/package=trend> (accessed October 2, 2021).
- Porter, S. E., Mosley-Thompson, E., Thompson, L. G., and Wilson, A. B. (2021). Reconstructing an interdecadal Pacific oscillation index from a Pacific basin-wide collection of ice core records. *J. Clim.* 34, 3839–3852. doi: 10.1175/JCLI-D-20-0455.1
- R Core Team (2018). *R: A Language and Environment for Statistical Computing*. Vienna: R Foundation for Statistical Computing.
- Rayner, N. A., Parker, D. E., Horton, E. B., Folland, C. K., Alexander, L. V., Rowell, D. P., et al. (2003). Global analyses of sea surface temperature, sea ice, and night marine air temperature since the late nineteenth century. *J. Geophys. Res.* 108:4407. doi: 10.1029/2002JD002670
- Reis, M., Graça, P. M. L. A., Yanai, A. M., Ramos, C. J. P., and Fearnside, P. M. (2021). Forest fires and deforestation in the central Amazon: effects of landscape and climate on spatial and temporal dynamics. *J. Environ. Manage.* 88:112310. doi: 10.1016/j.jenvman.2021.112310
- Resende, A. F., Nelson, B. W., Flores, B. M., and Almeida, D. R. A. (2014). Fire damage in seasonally flooded and upland forests of the Central Amazon. *Biotropica* 46, 643–646. doi: 10.1111/btp.12153
- Resende, A. F., Piedade, M. T. F., Feitosa, Y. O., Andrade, V. H. F., Trumbore, S., Durgante, F. M., et al. (2020). Flood-pulse disturbances as a threat for long-living Amazonian trees. *New Phytol.* 227, 1790–1803. doi: 10.1111/nph.16665
- Ribeiro, B. G. (1995). *Os Índios das Águas Pretas: Modo de Produção e Equipamento Produtivo*. São Paulo: Companhia das Letras/Edusp.
- Ribeiro, M. N. G., and Villa Nova, N. A. (1979). Estudos climatológicos da Reserva Florestal Ducke, Manaus, AM. III. Evapotranspiração. *Acta Amazon.* 9, 305–309.
- Richter, B. D., Baumgartner, J. V., Powell, J., and Braun, D. P. (1996). A method for assessing hydrologic alteration within ecosystems. *Conserv. Biol.* 10, 1163–1174. doi: 10.1046/j.1523-1739.1996.10041163.x
- Ritter, C. D., Andretti, C. B., and Nelson, B. W. (2012). Impact of past forest fires on bird populations in flooded forests of the Cuini river in the Lowland Amazon. *Biotropica* 44, 449–453. doi: 10.2307/23273137
- Rivera, J. D., Davies, G. M., and Jahn, W. (2012). Flammability and the heat of combustion of natural fuels: a review. *Combust. Sci. Technol.* 184, 224–242. doi: 10.1080/00102202.2011.630332
- Salati, E., and Vose, P. B. (1984). Amazon basin: a system in equilibrium. *Science* 225, 129–138. doi: 10.1126/science.225.4658.129
- Sampaio, P. M. (2003). Cidades desaparecidas na Amazônia Portuguesa. Póies, séculos XVIII e XIX. *Hist. Soc.* 10, 73–100.
- Sanford, R. L. Jr., Saldarriaga, J., Clark, K. E., Uhl, C., and Herrera, M. (1985). Amazon rainforest fires. *Science* 227, 53–55. doi: 10.1126/science.227.46.53
- Santos, A. R., and Nelson, B. W. (2013). Leaf decomposition and fine fuels in floodplain forests of the Rio Negro in the Brazilian Amazon. *J. Trop. Ecol.* 29, 455–458. doi: 10.1017/S0266467413000485
- Schöngart, J., and Junk, W. J. (2007). Forecasting the flood-pulse in Central Amazonia by ENSO-indices. *J. Hydrol.* 335, 124–132. doi: 10.1016/j.jhydrol.2006.11.005
- Schöngart, J., and Junk, W. J. (2020). “Clima e hidrologia nas várzeas da Amazônia Central,” in *Várzeas Amazônicas: Desafios para um Manejo Sustentável*, eds W. J. Junk, M. T. F. Piedade, F. Wittmann, and J. Schöngart (Manaus: Editora INPA), 44–65.
- Schöngart, J., Junk, W. J., Piedade, M. T. F., Ayres, J. M., Hüttermann, A., and Worbes, M. (2004). Teleconnection between tree growth in the Amazonian floodplains and the El Niño–Southern oscillation effect. *Glob. Change Biol.* 10, 683–692. doi: 10.1111/j.1529-8817.2003.00754.x
- Schöngart, J., Piedade, M. T. F., Ludwigshausen, S., Horna, V., and Worbes, M. (2002). Phenology and stem-growth periodicity of tree species in Amazonian

- floodplain forests. *J. Trop. Ecol.* 18, 581–597. doi: 10.1017/S0266467402002389
- Schöngart, J., Wittmann, F., Junk, W. J., and Piedade, M. T. F. (2017). Vulnerability of Amazonian floodplains to wildfires differs according to their typologies impeding generalizations. *Proc. Natl. Acad. Sci. U.S.A.* 114, 8550–8551. doi: 10.1073/pnas.1713734114
- Schöngart, J., Wittmann, F., Resende, A. F., Assahira, C., Lobo, G. S., Neves, J. R. D., et al. (2021). The shadow of the Balbina dam: a synthesis of over 35 years of downstream impacts on floodplain forests in Central Amazonia. *Aquat. Conserv.* 31, 1117–1135. doi: 10.1002/aqc.3526
- Silva, S. S., Oliveira, I. S., Morello, T. F., Anderson, L. O., Karlokoski, A., Brando, P. M., et al. (2021). Burning in southwestern Brazilian Amazonia, 2016–2019. *J. Environ. Manage.* 286:112189. doi: 10.1016/j.jenvman.2021.112189
- Sombroek, W. (1984). “Soils of the Amazon region,” in *The Amazon (Monographiae Biologicae)*, ed. H. Sioli (Dordrecht: Springer), 521–538.
- Sombroek, W. (2001). Spatial and temporal patterns of Amazon rainfall. *Ambio* 30, 388–396. doi: 10.1579/0044-7447-30.7.388
- Stahle, D. W., Cook, E. R., Burnette, D. J., Villanueva, J., Cerano, J. N., Burns, J., et al. (2016). The Mexican drought atlas: tree-ring reconstructions of the soil moisture balance during the late pre-Hispanic, colonial, and modern eras. *Quat. Sci. Rev.* 149, 34–60. doi: 10.1016/j.quascirev.2016.06.018
- Sternberg, H. O. (1987). Aggravation of floods in the Amazon river as a consequence of deforestation? *Geogr. Ann.* 69A, 201–219. doi: 10.2307/521378
- Targhetta, N., Kesselmeier, J., and Wittmann, F. (2015). Effects of the hydroedaphic gradient on tree species composition and aboveground wood biomass of oligotrophic forest ecosystems in the central Amazon basin. *Folia Geobot.* 50, 185–205. doi: 10.1007/s12224-015-9225-9
- ter Steege, H., Prado, P. I., Lima, R. A. F., Pos, E., Coelho, L. S., Lima Filho, D. A., et al. (2020). Biased-corrected richness estimates for the Amazonian tree flora. *Sci. Rep.* 10:10130. doi: 10.1038/s41598-020-66686-3
- Thorntwaite, C. W. (1948). An approach toward a rational classification of climate. *Geogr. Rev.* 38, 55–94. doi: 10.2307/210739
- Uhl, C., Kauffman, J. B., and Cummings, D. L. (1988). Fire in the Venezuelan Amazon 2: environmental conditions necessary for forest fires in the evergreen rainforest of Venezuela. *Oikos* 53, 176–184. doi: 10.2307/3566060
- Valle, R. B. M. (2012). *Mentes Graníticas e Mentes Areníticas. Fronteira Geo-Cognitiva nas Gravuras Rupestres do Baixo Rio Negro, Amazônia Setentrional*. Ph.D. Dissertation. São Paulo: Museu de Arqueologia e Etnologia da Universidade de São Paulo.
- Vance, T., Roberts, J., Plummer, C., Kiem, A., and van Ommen, T. (2015). Interdecadal Pacific variability and Australian mega-droughts over the last millennium. *Geophys. Res. Lett.* 42, 129–137. doi: 10.1002/2014GL062447
- Waldhoff, D., and Furch, B. (2002). Leaf morphology and anatomy in eleven tree species from Central Amazonian floodplains (Brazil). *Amazoniana* 17, 79–94.
- Wang, X., and Liu, H. (2016). PDO modulation of ENSO effect on tropical cyclone rapid intensification in the western North Pacific. *Clim. Dyn.* 46, 15–28. doi: 10.1007/s00382-015-2563-8
- Wantzen, K. M., Yule, C. M., Mathooko, J. M., and Pringle, C. M. (2008). “Organic matter processing in tropical streams,” in *Aquatic Ecology, Tropical Stream Ecology*, ed. D. Dudgeon (London: Academic Press), 43–64.
- Williams, E., Antonia, A. D., Antonia, V. D., Almeida, J. D., Suarez, F., Liebmann, B., et al. (2005). The drought of the century in the Amazon basin: an analysis of the regional variation of rainfall in South America in 1926. *Acta Amazon.* 35, 231–238. doi: 10.1590/S0044-59672005000200013
- Wittmann, F., Householder, E., Wittmann, A. O., Lopes, A., Junk, W. J., and Piedade, M. T. (2015). Implementation of the Ramsar convention on South American wetlands: an update. *Res. Rep. Biodivers. Stud.* 4, 47–58. doi: 10.2147/RRBS.S64502
- Wittmann, F., and Junk, W. J. (2016). “The Amazon river basin,” in *The Wetland Book II: Distribution, Description and Conservation*, eds C. M. Finlayson, G. R. Milton, R. C. Prentice, and N. C. Davidson (Heidelberg: Springer Verlag), 1–20.
- Wittmann, F., Schöngart, J., and Junk, W. J. (2010). “Phytogeography, species diversity, community structure and dynamics of central Amazonian floodplain forests,” in *Amazonian Floodplain Forests. Ecological Studies (Analysis and Synthesis)*, eds W. J. Junk, M. T. F. Piedade, F. Wittmann, J. Schöngart, and P. Parolin (Dordrecht: Springer), 61–102.

**Conflict of Interest:** The authors declare that the research was conducted in the absence of any commercial or financial relationships that could be construed as a potential conflict of interest.

**Publisher’s Note:** All claims expressed in this article are solely those of the authors and do not necessarily represent those of their affiliated organizations, or those of the publisher, the editors and the reviewers. Any product that may be evaluated in this article, or claim that may be made by its manufacturer, is not guaranteed or endorsed by the publisher.

Copyright © 2021 Carvalho, Wittmann, Piedade, Resende, Silva and Schöngart. This is an open-access article distributed under the terms of the Creative Commons Attribution License (CC BY). The use, distribution or reproduction in other forums is permitted, provided the original author(s) and the copyright owner(s) are credited and that the original publication in this journal is cited, in accordance with accepted academic practice. No use, distribution or reproduction is permitted which does not comply with these terms.